THE CRUSTAL STRUCTURE OF THE SCOTIA SEA FROM GEOMAGNETIC AND OTHER GEOLOGICAL INVESTIGATIONS

by
Loren W. Kroenke

A THESIS SUBMITTED TO THE GRADUATE DIVISION OF THE
UNIVERSITY OF HAWAII IN PARTIAL FULFILLMENT
OF THE REQUIREMENTS FOR THE DEGREE OF

MASTER OF SCIENCE

THE CRUSTAL STRUCTURE OF THE SCOTIA SEA FROM GEOMAGNETIC AND OTHER GEOLOGICAL INVESTIGATIONS

A THESIS SUBMITTED TO THE GRADUATE DIVISION OF THE
UNIVERSITY OF HAWAII IN PARTIAL FULFILLMENT
OF THE REQUIREMENTS FOR THE DEGREE OF

MASTER OF SCIENCE

GEOSCIENCES - GEOLOGY

JUNE 1968

By

Loren W. Kroenke

Thesis Committee:

George P. Woollard, Chairman
Gordon A. Macdonald
Alexander Malahoff
James Andrews

We certify that we have read this thesis and that in our opinion it is satisfactory in scope and quality as a thesis for the degree of Master of Science in Geosciences

THESIS COMMITTEE

George P. Woollard
Chairman

Alexander Malahoff

Gordon A. Macdonald

James E. Andrews

TABLE OF CONTENTS

Page

LIST OF TABLES

LIST OF FIGURES

Page

INTRODUCTION

During 1962 and 1963 the writer carried out a study of the magnetic field associated with the tectonic province defined by the Scotia Sea and Scotia Island Arc. The work was done under the direction of Dr. George P. Woollard and carried out on the USNS ELTANIN under National Science Foundation grant No. NSF-6-19611 to the University of Wisconsin.

The Scotia Sea is bounded on the east by the Scotia Arc and on the west by the Drake Passage (Fig. 1). The Scotia Arc consists of the North Scotia Ridge, the South Sandwich Islands and Trench, and the South Scotia Ridge. The Drake Passage lies between Tierra del Fuego and the Antarctic Peninsula. Also shown in Fig. 1 are the other prominent island groups which in conjunction with the South Sandwich Islands enclose two geologic sub-provinces--the East and West Scotia basins.

Historically, the region has been one of considerable geological and geophysical interest. Barrow (1831) was the first to suggest that the South Shetland Islands were a continuation of the cordillera of the Andes, and Suess (1909) made the remarkable prediction of a foredeep lying east of the South Sandwich Islands. Since then the tectonic origin of the Scotia Sea has been a subject of continuing speculation.

Over the years the region has repeatedly been the target of major research expeditions--the German METEOR (1925-1927) and the British DISCOVERY (1926-1939) investigations, among others, prior to the International Geophysical Year. Among the better-known reports that

Fig. 1. Chart of the Scotia Sea.

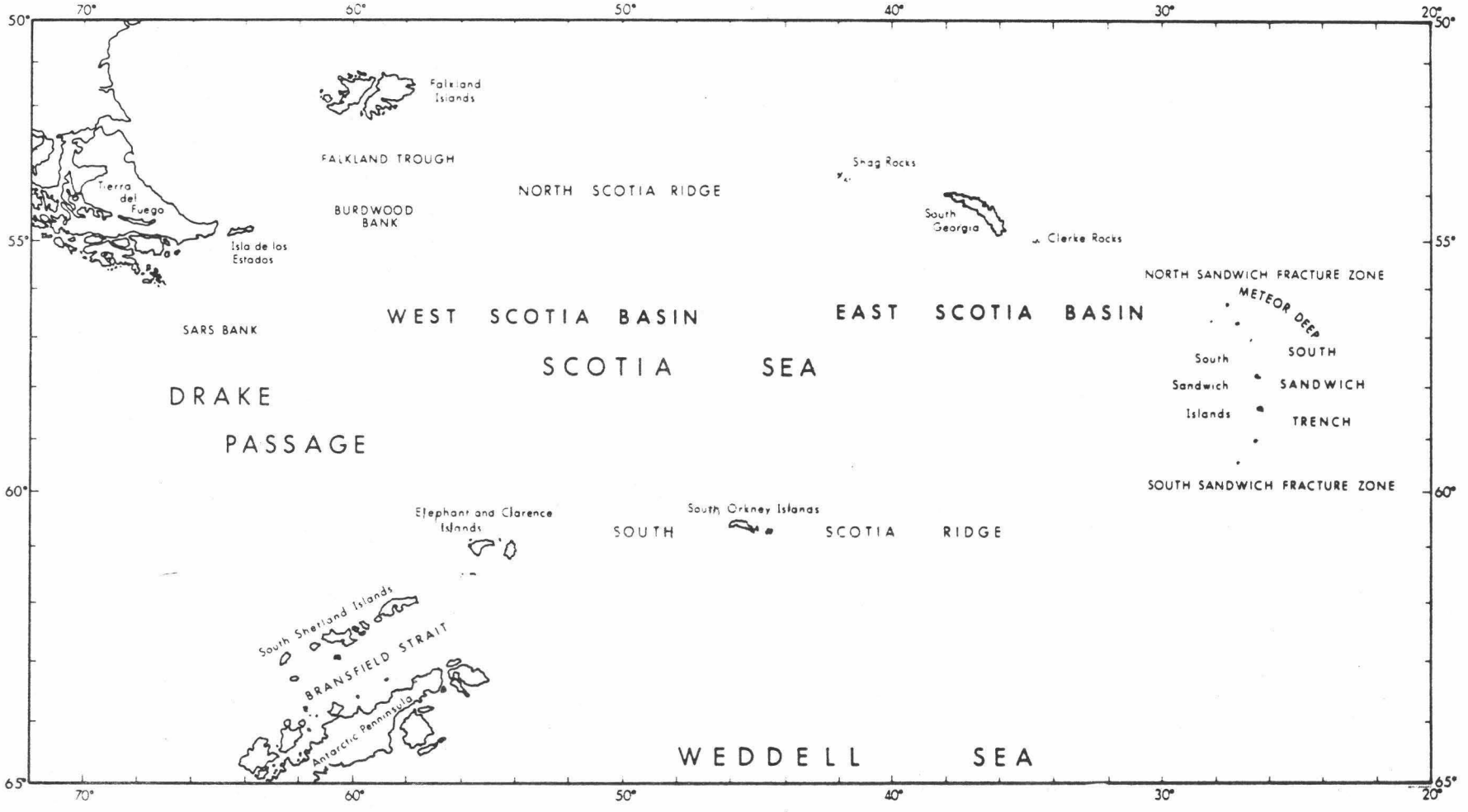
70°
60°
50°
40°
30°
20°
50°
55°
60°
65°
Falkland Islands
FALKLAND TROUGH
BURDWOOD BANK
NORTH SCOTIA RIDGE
Shag Rocks
South Georgia
Clerke Rocks
Tierra del Fuego
Isla de los Estados
SARS BANK
WEST SCOTIA BASIN
EAST SCOTIA BASIN
SCOTIA SEA
DRAKE PASSAGE
NORTH SANDWICH FRACTURE ZONE
METEOR DEEP
South Sandwich Islands
SOUTH SANDWICH TRENCH
SOUTH SANDWICH FRACTURE ZONE
Elephant and Clarence Islands
South Orkney Islands
SOUTH SCOTIA RIDGE
South Shetland Islands
BRANSFIELD STRAIT
Antarctic Peninsula
WEDDELL SEA

have appeared from geological exploration of the area are: Nordenskjöld (1910), Andersson (1906), Holtedahl (1929), Tilley (1930, 1935), Tyrrell (1921, 1930, 1945), Herdman (1948), Trendall (1953, 1959), Matthews (1959) and Hawkes (1962).

Although geophysical measurements other than bathymetry, notably the refraction investigations of Ewing and Ewing (1959), had been reported from the Scotia Sea prior to 1962, these were limited in extent and for the most part remain unpublished. There was little published or unpublished information concerning the magnetic field associated with the region. In 1959 the British Antarctic Survey (Griffiths and others, 1965) initiated long-range geophysical investigations of the Scotia Sea which included magnetic observations. Starting in 1962 and throughout 1963 the USNS ELTANIN engaged in comprehensive oceanographic studies of the area. These included phases of physical oceanography, marine biology, and marine geology as well as geophysics.

It was during this period that the writer conducted the present thesis study of the variation in the absolute value of the earth's magnetic field in the Scotia Sea from the USNS ELTANIN. The magnetic data were obtained using a proton precession magnetometer with a 6-second recycle rate, and a towed sensing coil. Measurements were obtained along approximately 20,000 miles of ship track.

The objective of the work was to obtain data which relate to crustal thickness and the geology of the crystalline basement in the Scotia Sea area. It was hoped to be able to map changes in lithology

of the basement rock complex and relate broad regional magnetic anomalies with susceptibility changes deep within the crust, correlating these, wherever possible, with observed seismic discontinuities. As will be shown later in the text, these objectives were for the most part achieved.

Acknowledgments

The author is indebted to the Captain and the crew of the USNS ELTANIN without whose cooperation this work would not be possible, and to the National Science Foundation representatives whose help and support is deeply appreciated. The technical assistance of members of the staff of Lamont Geological Observatory who aided in installing and initially servicing the magnetometer, and the logistic support furnished by members of the National Science Foundation, are sincerely acknowledged.

The contribution of the many people from the University of Wisconsin and the University of Hawaii, whose assistance and encouragement were invaluable in completing this work, is also gratefully recognized. In particular, thanks are due James Pew of the University of Wisconsin who operated the magnetometer on Cruises 9 and 10, and Lawrence Machesky, Shirley Machesky, and Karen Meagher of the University of Hawaii who assisted in the tabulating and checking of the data.

Finally, the unselfish effort of my colleagues at sea, representing many universities and research institutions, in maintaining the electronics lab watch can never be fully acknowledged.

INSTRUMENTATION, FIELD PROGRAM, AND PROCEDURE

Instrumentation

The USNS ELTANIN is the former Naval cargo vessel TAK-270 which was converted in 1962 by the National Science Foundation for survey work and scientific research in polar regions. The vessel is operated for the National Science Foundation by the Military Sea Transportation Service.

The total intensity proton precession magnetometer used was built by the Lamont Geological Observatory of Columbia University and based on the design of the prototype instrument developed by Varian Associates (Hirshman and Luskin, unpublished material). The performance of the instrument together with the results of the shakedown cruises are discussed by Kroenke and Woollard (Hawaii Institute of Geophysics research report, in preparation). The components of the system were as follows:

1. The lucite fish and coil assembly.

   The fish contained the coil assembly, immersed in distilled water, and consisted of two orthogonal coils of #10 copper wire wound in series and oriented normal to the vector of the ship's motion.

2. One thousand feet of towing cable supplied by the Simplex Wire and Cable Company, Cambridge, Massachusetts.

   The cable consisted of 2 conductors of #10 49-strand wire (polyethylene-jacketed) with a phosphor bronze braid and reinforced neoprene jacket; rated at 600 volts.

3. A program unit furnished by Lamont Geological Observatory.

   This unit, by means of motor-driven cams and microswitches, controlled the timing of the polarizing and the counting cycles of the magnetometer. It also reset and triggered the counting stages of the digital counter.

4. A pre-amplifier and amplifier constructed by Lamont Geological Observatory.

5. A Beckman/Berkeley Preset Universal EPUT and Timer, Model 7361 TR.

   This instrument, a digital counter capable of measuring period, performed the read-out function of the proton precession magnetometer. Its operation was comparable to the slow and fast gates of a Varian airborne magnetometer.

6. A Hewlett-Packard Digital to Analog Converter Model 3120-3.

   This unit converted the digitized signal from the EPUT meter to an analog form suitable for sampling by a Speedomax recorder.

7. A Leeds-Northrup Speedomax Recorder.

   This instrument was a potentiometer-type pen recorder with a paper speed of 12 inches per hour and a recording width of 10 inches. In March 1962 it was modified, by technicians from Lamont Geological Observatory, to accept

and record the signal from the Hewlett-Packard converter.

All the components with the exception of the fish and towing cable were mounted in the electronics laboratory in the forward section of the ship. During towing operations, the cable was secured around the gypsy head of the work winch and passed over the stern on the port side of the after platform. Prior to the beginning of Cruise 8 a winch was installed to mechanically stream and retrieve the towing cable.

Field Program

Cruises 1 and 2 of the ELTANIN were primarily of a shakedown nature, and together with Cruise 3 (New York to Valparaiso) are discussed elsewhere (Kroenke and Woollard, Hawaii Institute of Geophysics research report, in preparation). Upon completion of the first cruise in the Drake Passage (Cruise 4 in Fig. 2) the scientific party decided to extend the investigations to the east in order to include the entire Scotia Sea, a distinct physiographic province defined within the boundaries of the Scotia Arc. From July 1962 through December 1963 the ELTANIN, operating primarily out of Valparaiso, Chile, cruised in the Scotia Sea. The ship tracks in this area are shown in Fig. 2. The tabulated total intensity values and position, and the depth of water are given in Kroenke and Woollard (Hawaii Institute of Geophysics research report, in preparation).

Because of adverse weather conditions and the absence of LORAN facilities, it was expected that navigation would pose a major problem

Fig. 2. Cruise tracks of the USNS ELTANIN in the Scotia Sea, the South Pacific, and the South Atlantic (1962-1963).

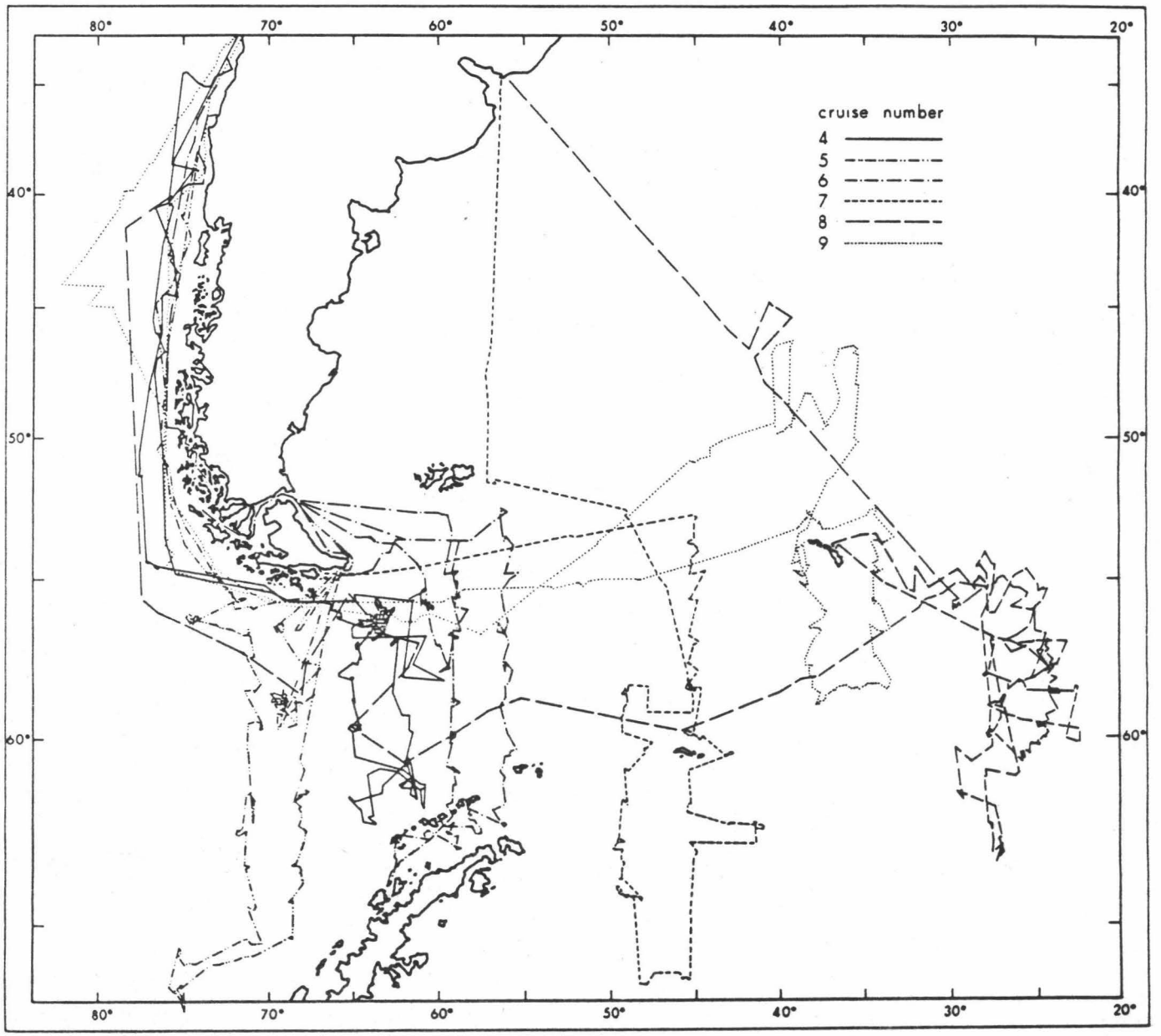
80°
70°
60°
50°
40°
30°
20°
40°
50°
60°
cruise number
4
5
6
7
8
9

in the south polar seas. However, an analysis of the data indicates that the navigation was of a higher order of accuracy than had been anticipated. In general, the navigational accuracy is estimated to be about ±5 miles; but observed discrepancies in the bathymetric and magnetic data at several track intersections indicate errors as great as ±10 miles were present at times.

Operating Procedure

While underway, the magnetometer sensing head (fish) was towed astern of the vessel at a distance varying between 500 and 1000 feet. Normally, during the approach to a scientific station (when the ship was hove to), the fish was retrieved preparatory to the over-the-side station activities. At certain times, however, the sensor was streamed while drifting, in order to monitor temporal magnetic field fluctuations.

A continuous electronics lab watch was maintained during the operation of the magnetometer and magnetic data were continuously recorded in analog form on the strip chart recorder. The record trace recorded the last three digits of the period of a predetermined (pre-set) number of precession cycles measured by the EPUT meter. The first three digits (regional values) were annotated directly on the record each hour together with Greenwich Civil Time, the pre-set value of the number of precession cycles included in the count period (comparable to the slow gate of the Varian magnetometer) and the date.

At appropriate intervals, the course, speed, and distance traveled in nautical miles (from the electro-magnetic log) and the depth in

fathoms (from the precision depth recorder) were also logged.

Since the values recorded on the analog recorder and visually presented on the digital counter were given in terms of period of a predetermined number of precession cycles, it was necessary to convert these values to absolute field strength in terms of gammas. After a roll of chart paper on the Speedomax recorder was filled, the time was scaled off in 15-minute intervals. The values were read at these intervals and also at maximum and minimum points and the total field strength calculated in gammas.

REDUCTION AND EVALUATION OF DATA

Data Reduction

The theory of the proton precession magnetometer has been presented by Waters and Francis (1958) and is based on the relationship

$$F = \frac{2\pi}{g'} \cdot f_p$$

where F is the absolute value of the total intensity of the magnetic field, g' is the gyromagnetic ratio for a proton, and f_p is the precession frequency. Thus F is directly proportional to f_p. The value of g' determined by the National Bureau of Standards (Driscoll and Bender, 1958), and later adopted by the International Association of Geomagnetism and Aeronomy (Nelson, 1960), is (2.67513 ± .00002) x 10^4 radians/gauss second. This gives 23.4873 gamma seconds/cycle for the value of $\frac{2\pi}{g'}$.

The data were reduced at the Geophysical and Polar Research Center of the University of Wisconsin and at the Hawaii Institute of Geophysics. The values of total intensity (F) were then tabulated with the time of observation, position, and depth of water. Depths were taken either directly from the precision depth recorder or from the plotted soundings prepared by Lamont Geological Observatory (1963-1965). In neither case were the data corrected for regional variations in the average vertical sound velocity (Heezen and others, 1959). As will be shown in the section on bathymetry, the error in depth from this cause does not exceed 2%.

Vessel Effects on Magnetic Measurements

During Cruises 1, 2, and 3 the magnetometer fish was towed astern of the ELTANIN at a distance of approximately 550 feet (two ship-lengths). At this distance the magnetic effect of the ship should have been less than 10 gammas (Bullard and Mason, 1961). At low geomagnetic latitudes during Cruise 3, however, circular maneuvers, designed to reveal possible magnetic effects of the vessel at different headings, disclosed that the effect was somewhat greater, possibly as much as 50 gammas greater. During Cruises 4 through 8--in an effort to decrease the heading effect--the towing distance was increased to between 750 and 1,000 feet.

Other minor magnetic effects from bathythermograph (BT) operation and trawling were observed, but for the most part, these resulted in disturbances of less than 10 gammas in the magnetic field intensity measurements. Recurring line-voltage fluctuations varying between 85 and 135 volts--as a result of heavy current drains by winch and deck equipment operation and by switching of generators--frequently were troublesome. The effect of this on the magnetometer could not be completely analyzed, but erratic instrument behavior was observed. During Cruise 3, voltage regulation equipment was incorporated into the circuit to suppress most of this type of variation, and resulted in more precise data and prolonged life of the electronic components of the magnetometer.

Temporal Magnetic Disturbances

Since the magnitude of diurnal and other temporal changes in the

magnetic field is known to vary from one area to another, it was realized that any attempt to remove the effect of temporal fluctuations, as recorded at observatories which were far from the area of investigation, could introduce significant errors. Therefore, no corrections for temporal variation in the earth's magnetic field have been applied to the data. However, K indices were examined in order to aid in distinguishing large temporal fluctuations from spatial variations. For the cruises in the Scotia Sea (Cruises 4 through 9), K indices from individual observatories were utilized in analyzing the data. In addition, for Cruises 2 through 10, geomagnetic planetary 3-hour-range indices (K_p) (Lincoln, 1962-1964) were also examined for the periods of observation. According to convention, the K indices are whole integers between 0 and 9, indicating the difference between maximum and minimum values of one component of the magnetic intensity vector during a 3-hour period. The gamma range of the K indices varies between observatories, and a quantitative value for the K index exists only with reference to the particular observatory issuing the index. In general, comparison of the K indices with a particular period of observation furnished a simple, but qualitative, measure of reliability for the data recorded during that period. The data used in the detailed analysis were all obtained during periods of relative quiescence.

MAGNETIC ANOMALIES OVER THE SCOTIA SEA

The Total Intensity Magnetic Field

After the Scotia Sea magnetic data had been reduced, as previously described, plots were made of the total intensity values for the position of the USNS ELTANIN as reported in the ELTANIN Data Sheets (1962-1963), and contoured in intervals of 100 gammas. The resulting total intensity chart is shown in Fig. 3. As can be deduced from the numerous dashed lines, this contoured chart is not as well controlled as one would wish. Annual change for this region as determined from the U. S. Naval Oceanographic Office chart H. O. 1703 (1965) varies between -70 and -115 gammas per year. This is close to the figure of -120 gammas per year derived and used by Griffiths and others (1965). However, as the ELTANIN data were acquired only between July 1962 and December 1963 (a period of slightly less than 18 months duration) and because navigational inconsistencies and our inability to remove the effect of short-term temporal variations gave a larger uncertainty in values, no corrections were applied to the data for secular variation.

As shown by Fig. 3, the regional gradient resulting from the earth's main field tends to suppress and obscure the effect due to buried geologic bodies. In order to evaluate the tectonic pattern of the area, it was necessary to construct a smoothed representation of the regional field which was subtracted from the total field before undertaking a geologic analysis of the results.

The Regional Magnetic Field

The quantity and areal distribution of the ELTANIN data did not appear to warrant the use of elaborate procedures for determining the

Fig. 3. Magnetic total intensity chart of the Scotia Sea (1962-1963). Contour interval, 100 gammas.

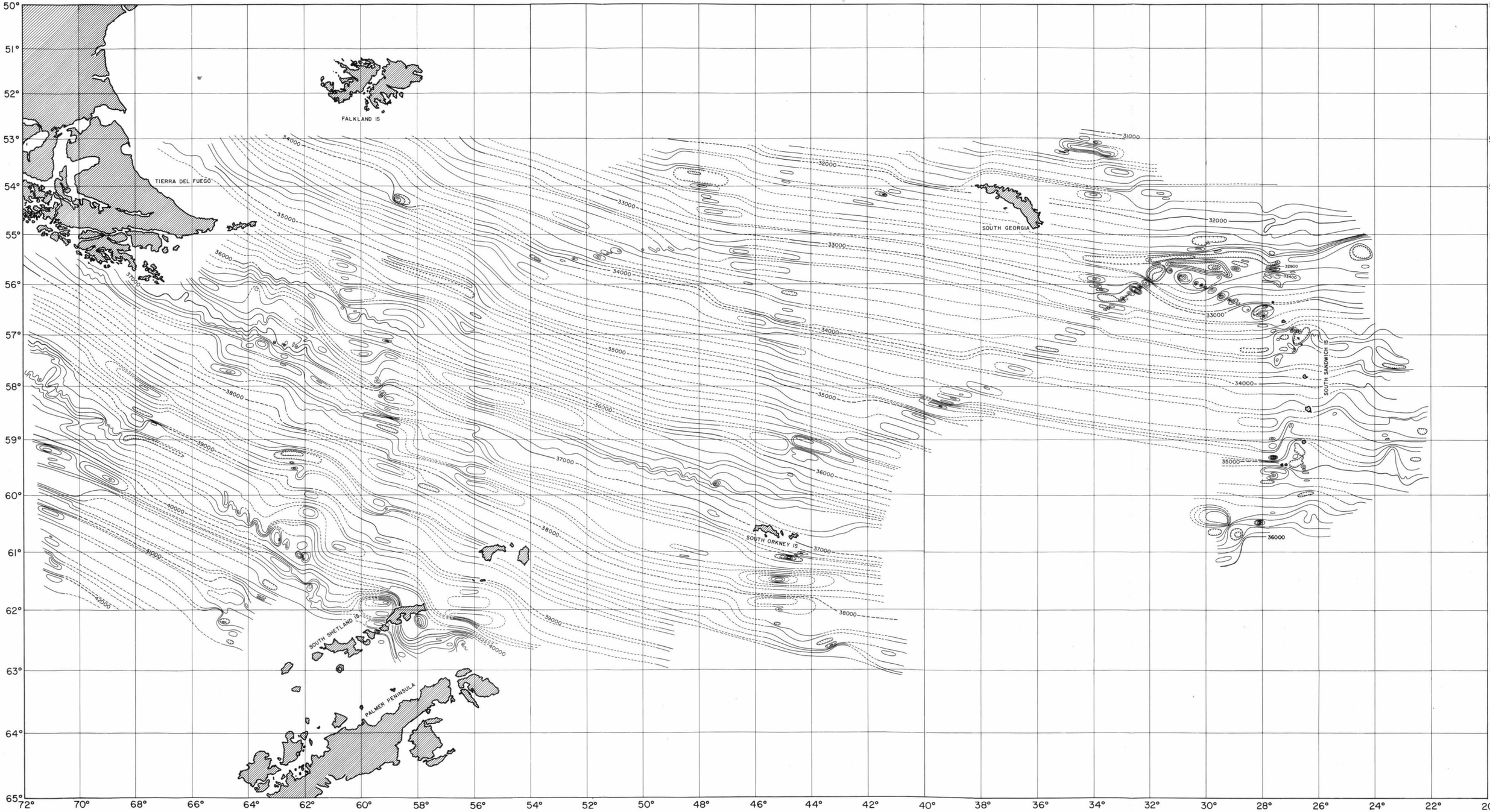
FALKLAND IS
TIERRA DEL FUEGO
SOUTH GEORGIA
SOUTH SANDWICH IS
SOUTH ORKNEY IS
SOUTH SHETLAND IS
PALMER PENINSULA
31000
32000
33000
34000
35000
36000
37000
38000
39000
40000
41000
42000
32800
33400
50°
51°
52°
53°
54°
55°
56°
57°
58°
59°
60°
61°
62°
63°
64°
65°
72°
70°
68°
66°
64°
62°
60°
58°
56°
54°
52°
50°
48°
46°
44°
42°
40°
38°
36°
34°
32°
30°
28°
26°
24°
22°
20°

regional gradient, such as those discussed by Wold and Wolfe (1966), and therefore, the total intensity contours (Fig. 3) were visually smoothed to define the regional magnetic field (Fig. 4).

Comparison of the chart in Fig. 4 with the U. S. Naval Hydrographic Office chart H. O. 1703 (1955), corrected to 1963, disclosed large discrepancies. However, comparison with the regional chart of the Scotia Sea published by Griffiths and others (1965) showed there was reasonable agreement. There are slight differences in the South Sandwich Islands, but these can be attributed to the fact that the amount of data available to the writer was greater than was available to Griffiths. Later, the validity of the writer's regional magnetic field chart was further substantiated by the close agreement with the newly released chart H. O. 1703 (1965) based on the results of a spherical harmonic analysis to degree and order 12 (Fig. 5).

The Residual Magnetic Field

The residual magnetic field chart presented in Fig. 6 was obtained by the relatively simple method of subtracting the regional contour values from the total intensity contour values. Although the validity of the resulting residual anomalies based on relatively few data and a non-uniform distribution of observations is open to question, no significant geologic analysis could be undertaken without the removal of the regional gradient. The smoothed residual field shown in Fig. 6 is believed to portray the magnetic anomaly pattern to a first approximation. The field portrayed represents the composite effect of anomaly sources at various depths in juxtaposition.

Fig. 4. Regional magnetic intensity chart of the Scotia Sea (1962-1963). Contour interval, 500 gammas.

FALKLAND IS

TIERRA DEL FUEGO

SOUTH GEORGIA

SOUTH SANDWICH IS

SOUTH ORKNEY IS

SOUTH SHETLAND IS

PALMER PENINSULA

32000

33000

34000

35000

36000

37000

38000

39000

40000

41000

42000

50° S
51°
52°
53°
54°
55°
56°
57°
58°
59°
60°
61°
62°
63°
64°
65°

72° W
70°
68°
66°
64°
62°
60°
58°
56°
54°
52°
50°
48°
46°
44°
42°
40°
38°
36°
34°
32°
30°
28°
26°
24°
22°
20°

Fig. 5. Regional magnetic intensity chart of the Scotia Sea, after Oceanographic Office Chart No. 1703 (1965). Contour interval, .01 oersted.

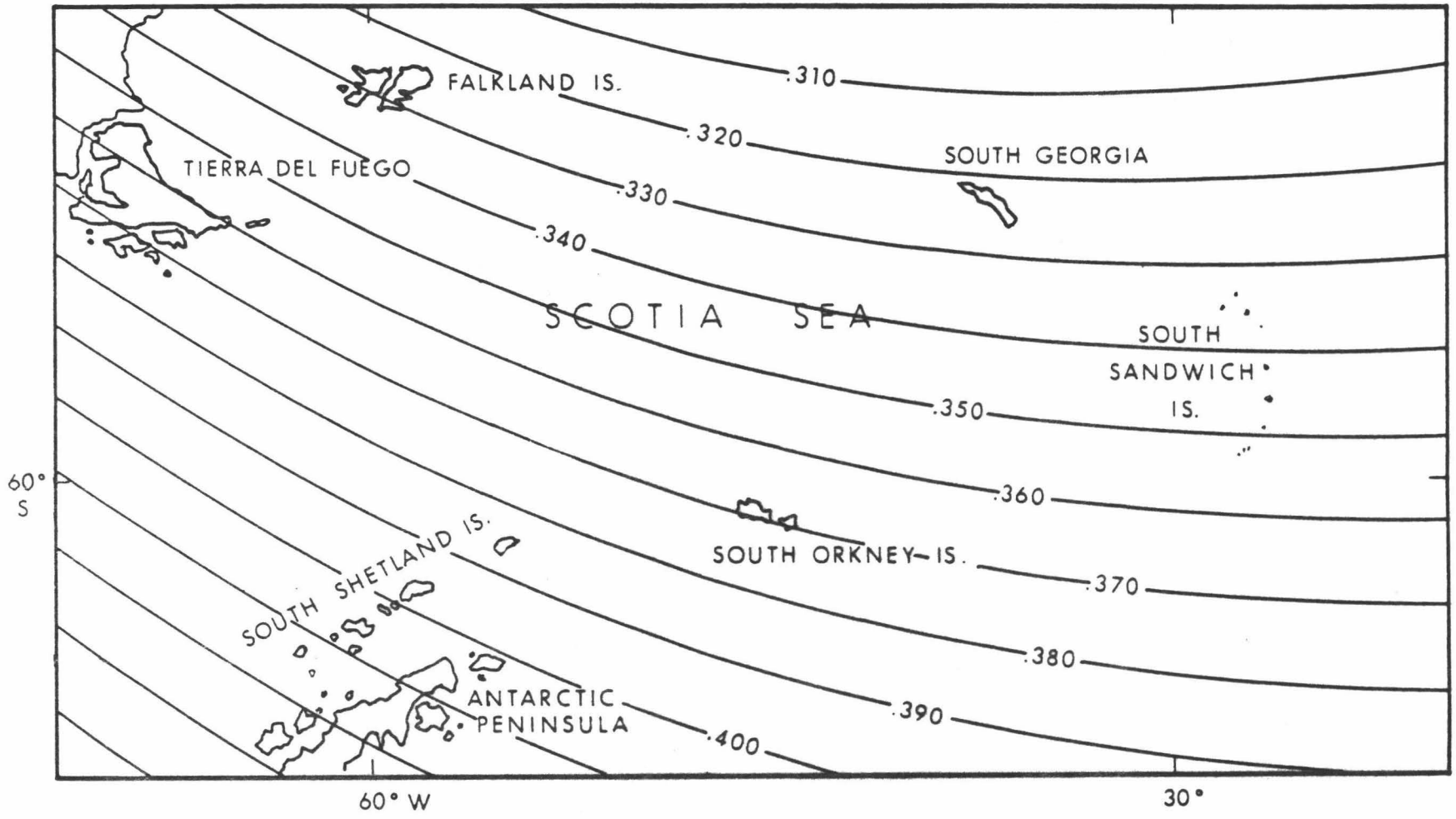
FALKLAND IS.
TIERRA DEL FUEGO
SOUTH GEORGIA
SCOTIA SEA
SOUTH SANDWICH IS.
SOUTH ORKNEY IS.
SOUTH SHETLAND IS.
ANTARCTIC PENINSULA
310
320
330
340
350
360
370
380
390
400
60° S
60° W
30°

Fig. 6. Residual magnetic anomaly chart of the Scotia Sea (1962-1963). Contour interval, 100 gammas.

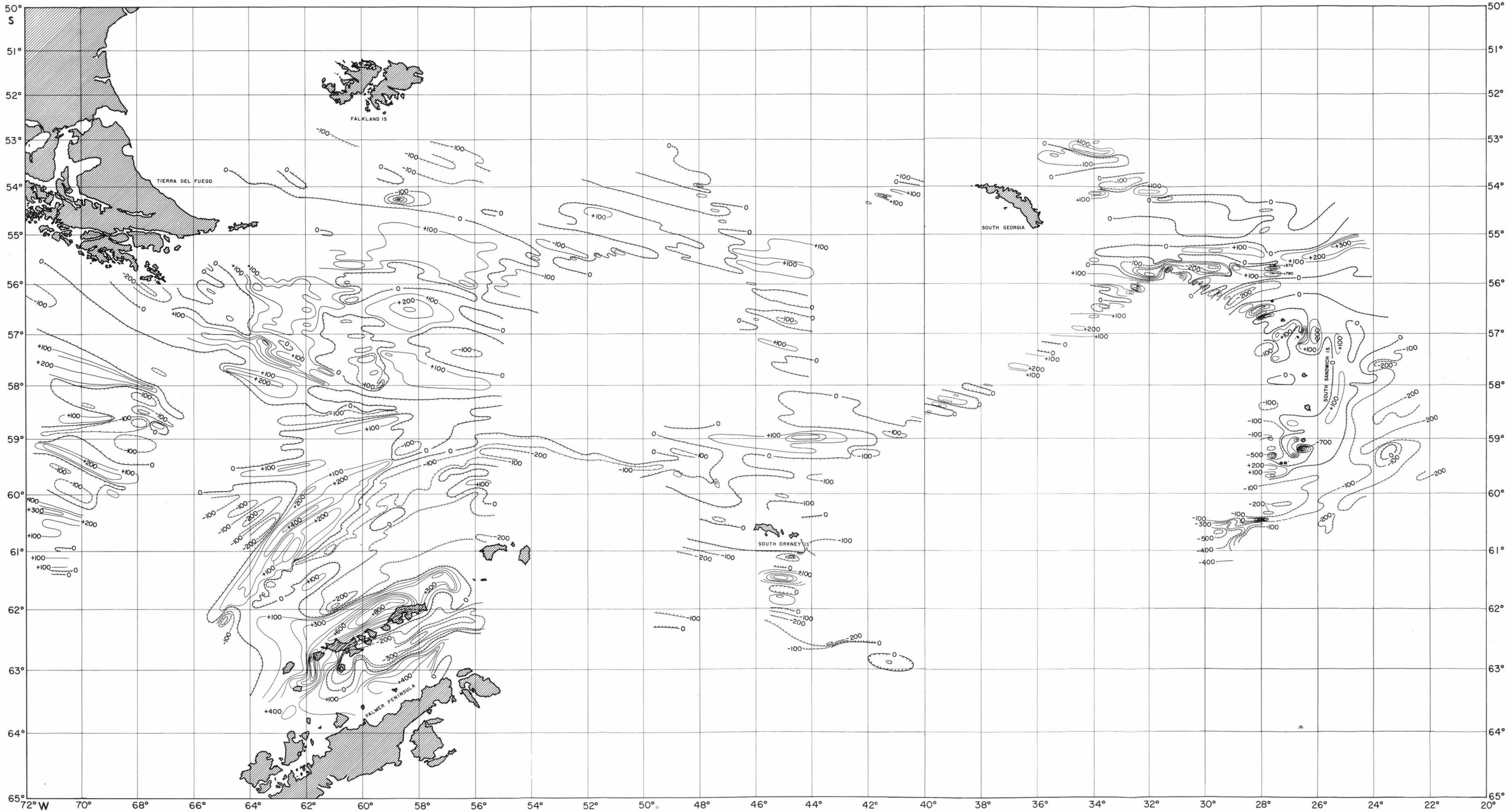
FALKLAND IS
TIERRA DEL FUEGO
SOUTH GEORGIA
SOUTH SANDWICH IS.
SOUTH ORKNEY IS.
PALMER PENINSULA
50° S
51°
52°
53°
54°
55°
56°
57°
58°
59°
60°
61°
62°
63°
64°
65°
72° W
70°
68°
66°
64°
62°
60°
58°
56°
54°
52°
50°
48°
46°
44°
42°
40°
38°
36°
34°
32°
30°
28°
26°
24°
22°
20°

Although some spatial aliasing in contouring the residual data could not be avoided, which biased the results to some extent, a comparison of the writer's residual values for the Bransfield Strait area with those determined by Griffiths and others (1965) for the same area show excellent agreement, both in magnitude and in geometry. This allowed incorporation of these data with those of the writer (Fig. 6) with almost no adjustment. The inclusion of these data considerably extended the areal coverage of the data analyzed.

The prevalent system of lineations of residual anomalies paralleling the Scotia Arc and internal topographic elements is more clearly delineated in the bipole trend chart of Fig. 7. The solid lines represent positive anomaly lineations while the dotted lines show the negative anomaly trends. The most striking, though possibly somewhat conjectural, aspect of the chart is the apparent convergence of anomaly lineations within the Drake Passage. The significance of this will be discussed later.

Examination of Figs. 6 and 7 focuses attention on the following features:

1. The North Scotia Ridge.

The absence of any continuous or noticeable high amplitude, long wavelength anomalies associated with or adjacent to the North Scotia Ridge is of considerable interest. Griffiths and others (1965) arrived at a similar result and describe the lack of magnetic anomalies associated with the Ridge as one of the main features that emerges from consideration of the Scotia Arc. They refer to "the continuation

Fig. 7. Magnetic bipole trend chart of the Scotia Sea. Solid lines indicate positive magnetic anomaly trends; dashed lines, negative trends.

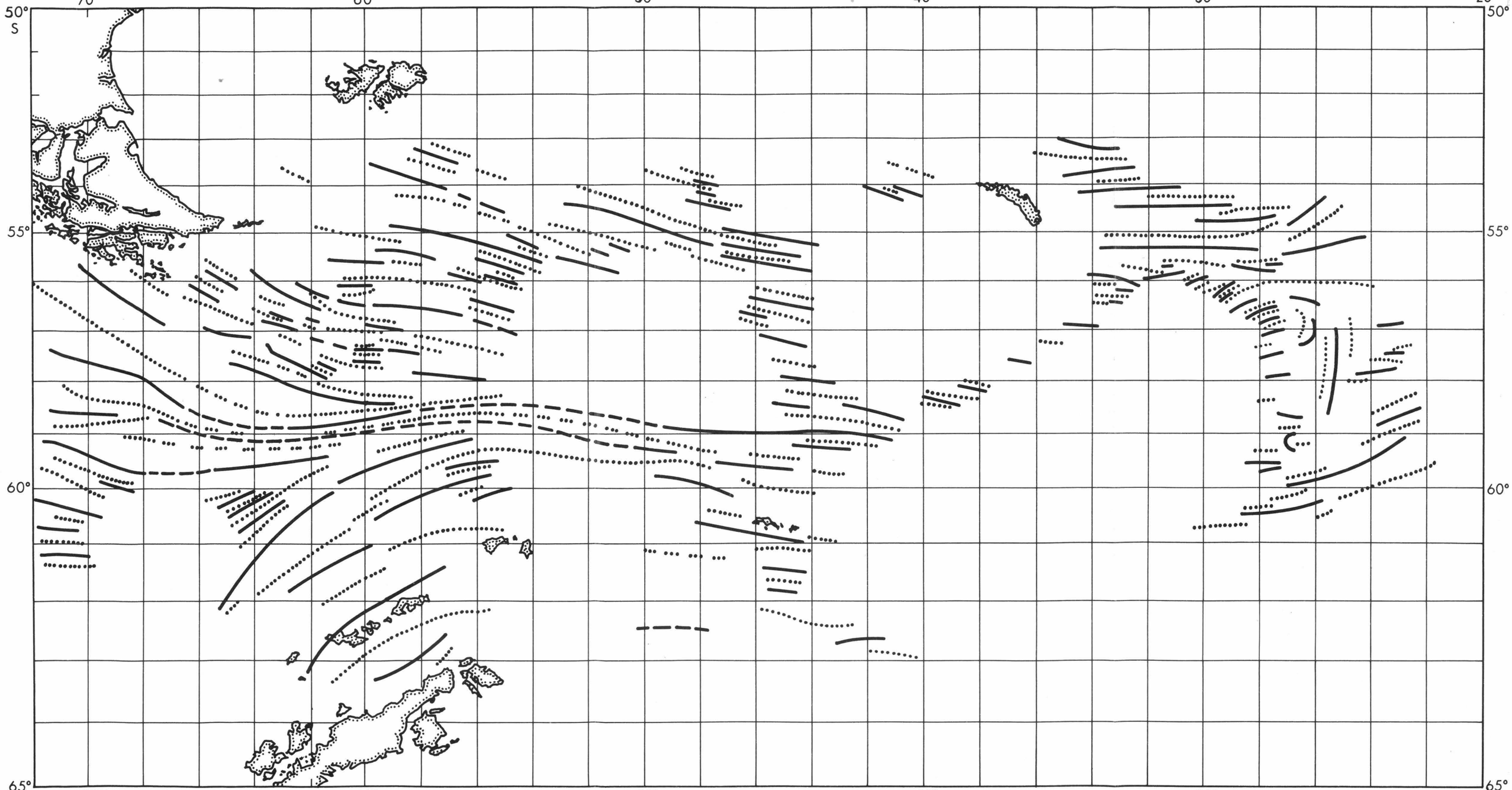
70°
60°
50°
40°
30°
20°
50° S
55°
60°
65°
70° W
60°
50°
40°
30°
20°
50°
55°
60°
65°

of the submarine ridge from the Burdwood Bank to South Georgia as a non-magnetic structure." This observation is in agreement with the seismic refraction measurements of Ewing and Ewing (1959), which indicate that the main crustal layer is depressed about 5 kilometers under the ridge and that the Burdwood Bank is composed mainly of consolidated sediments.

2. The North and South Sandwich Fracture Zones.

The elongated anomaly pattern at the northern extremity of the South Sandwich Trench seems to coincide with the fractured area described by Heezen and Johnson (1965). Significantly, the anomaly extends considerably farther to the east beyond the disturbed area indicated by the bottom relief. This suggests that the structure is much more extensive than the bathymetric data indicate. This situation is probably analogous to that described by Malahoff and Woollard (1966) who traced the Molokai Fracture Zone, as delineated by magnetic anomalies, through the Hawaiian Archipelago, and it will be discussed further under bathymetry of the Scotia Sea.

Heezen and Johnson (1965) first described the well developed South Sandwich Fracture Zone at the southern end of the South Sandwich Trench. As will be shown later in the section on bathymetry, this topographic feature extends considerably to the east--in effect paralleling the magnetic anomaly associated with the North Sandwich Fracture Zone. Like the northern structure, the South Sandwich Fracture Zone is also anomalous, but, in this case, the areal extent of the magnetic anomaly cannot be determined because of insufficient data.

3. The South Sandwich Trench.

The residual field over the South Sandwich Trench and associated South Sandwich Island Arc roughly reflects the tectonic fabric of the region. Although no local or regional magnetic anomalies of large amplitude are found in association with the Trench itself, an anomaly of very low amplitude and long wavelength appears to parallel the trench axis, possibly originating at great depth, but, conceivably being due to the topographic effect of the trench. Numerous magnetic anomalies of high amplitude and short wavelength appear to be associated with the volcanic features in the shallower water areas adjacent to the island arc. In addition, numerous local anomalies exist over the deeper water areas along the northwest extension of the island arc in the East Scotia Basin. They appear to decrease in magnitude and increase in wavelength westward to the Scotia Basin, suggesting a progressive increase in depth of the source of the anomalies to the west.

4. The South Scotia Ridge.

Although the conclusion is based on a relatively small number of observations, the South Scotia Ridge in contrast to the North Scotia Ridge appears to be characterized by pronounced magnetic anomalies. Shallow (short wavelength) anomalies superimposed on deep (long wavelength) anomalies culminate to the west in the high amplitude (-400 to +800 gammas) Bransfield Strait anomaly centered over the South Shetland Islands.

Griffiths and others (1965) have discussed the structural interpretation of the Bransfield Strait. In this region they fitted the

observed magnetic anomaly field with a two-dimensional model, modified slightly from their gravity and seismic models. The inclination was assumed to be 58° and the susceptibility contrast approximately 6×10^{-3} cgs units. Their interpretation is shown in Fig. 8; it will be discussed in the section on seismic refraction measurements.

Fig. 8. Gravity and magnetic profiles across the Bransfield Strait. The densities are based on known seismic velocities; the inclination of magnetization is assumed to be 58°, and the apparent susceptibility contrast, approximately 6×10^{-3} emu/cm^3 (after Griffiths and others, 1965). Distance are in kilometers.

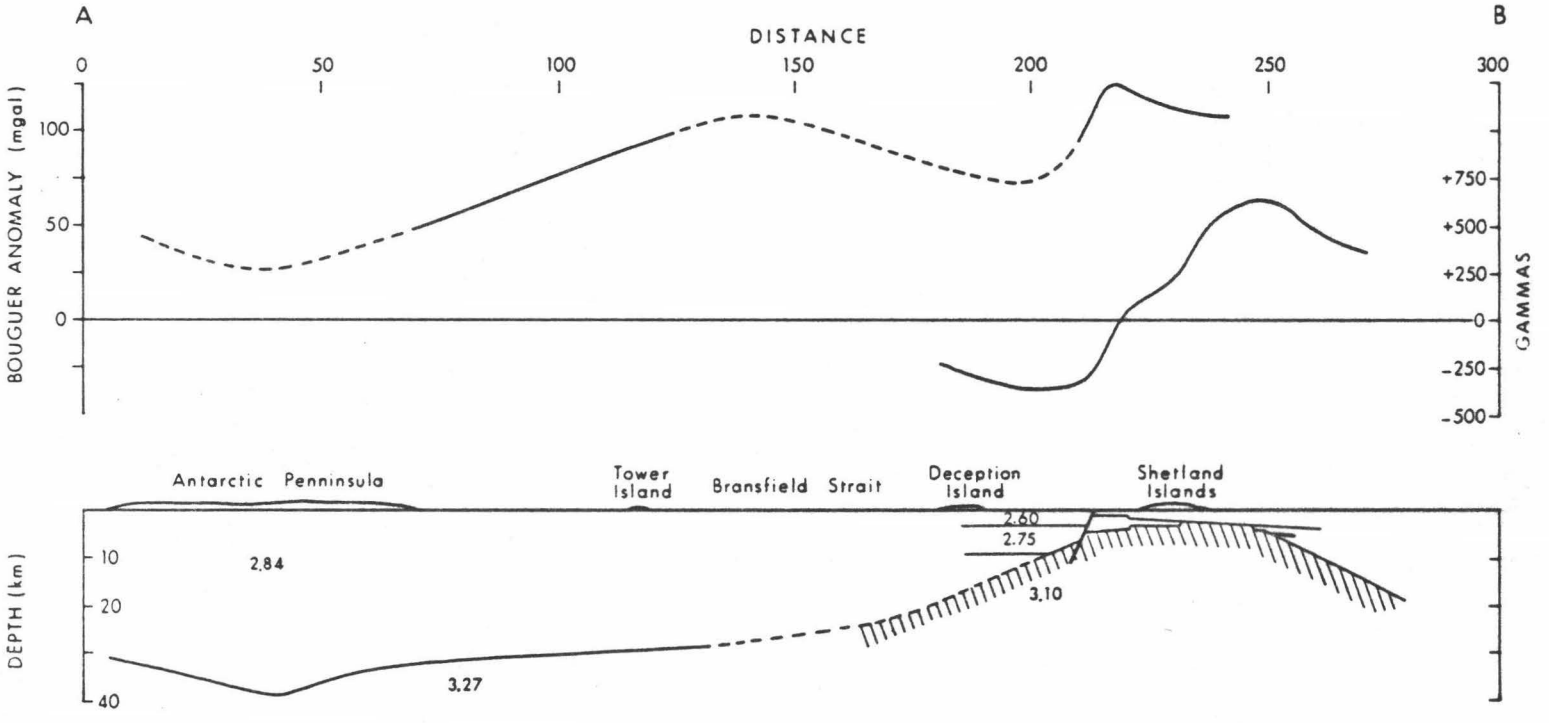
A
B
DISTANCE
0
50
100
150
200
250
300
BOUGUER ANOMALY (mgal)
100
50
0
+750
+500
+250
0
-250
-500
GAMMAS
Antarctic Penninsula
Tower Island
Bransfield Strait
Deception Island
Shetland Islands
DEPTH (km)
10
20
40
2.84
2.60
2.75
3.10
3.27

SOURCE OF THE MAGNETIC ANOMALIES

The Effect of Terrain

The relationship between magnetic anomalies and topographic relief has been investigated by several writers. Nettleton (1940), in discussing the effect of relief on buried magnetic basement, points out that the contribution to the magnetic anomaly of buried topography is often negligible compared to the contribution of contrasts in magnetization extending to great depths (vertical intrusive bodies). Nettleton has calculated that a maximum anomaly of 150 gammas in vertical intensity may be expected from a structural relief whose elevation is one-quarter of its depth of burial and having a vertical polarization with a contrast of 0.003 cgs units. This calculation is based on the assumption of a vertical-walled structure, long in the direction perpendicular to the magnetic profile, and any decrease in the slope of the walls would decrease the amplitude of the anomaly.

Griffiths and others (1965), in considering the effect of topographic relief in the Scotia Sea, observed that "there is, in general, no obvious relationship between the magnetic features and the observed bottom topography," and as a result they presume that in many places the igneous rock is buried beneath sedimentary blanket. They also state that in order to approximate topography with triangular blocks, a magnetization contrast (apparent susceptibility or K_A) of 3×10^{-3} cgs units is required, suggesting basic rock material with marked remanence (J_r). Furthermore, in one of the few places where correlation appeared possible, a magnetization contrast of 5×10^{-3} cgs units was required in order to obtain good agreement between the

calculated and observed anomalies due to the observed topography.

The relation of the apparent susceptibility to the total field intensity is given by (Nagata, 1961)

$$J = k H_o + J_n \simeq K_A H_o$$

where J is the intensity of magnetization, k is the magnetic susceptibility, H_o is the strength (intensity) of the present field, J_n is the in situ natural remanent magnetization (assuming that remanent magnetization is roughly in the direction of the present field), and K_A is the apparent susceptibility or magnetization contrast, and

$$K_A = k(1 + Q)$$

where Q is the Königsberger ratio

$$Q_n \equiv J_n/k H_o$$

Since for most lithologies which are to be considered in this discussion Q is generally greater than or equal to 10, then

$$K_A \simeq k Q = J_n/H_o$$

Following common usage J_r (measured remanent magnetization) will be substituted for J_n and average magnetic field intensity F is

substituted for H_o. Thus

$$K_A \simeq J_r/F$$

From the foregoing discussion it is apparent that although susceptibility (k) can often be neglected, values for natural remanent magnetization (J_r) must be known in order to estimate the effect of topographic relief. J_r measurements of rocks from the Scotia Sea area are not available; consequently, the assignment of values to magnetization contrasts (K_A) is conjectural and involves assumptions as to the nature of the sea floor. This leaves no alternative but to estimate the K_A from an analysis of the magnetic profiles. This analysis, in turn, depends upon the validity of the model chosen to represent the anomalous body.

Method of Analysis

The various techniques of quantitatively interpreting magnetic data have recently been reviewed and evaluated by several writers. Sankar-Narayan (1961) presents a comprehensive evaluation of many of the most common methods of computing depths to structures causing anomalies. Ostenso (1962), working in Arctic latitudes near the north magnetic pole, extended the discussion, but concentrated on the half-slope method of Peters (1949) for determining depths. His results suggest considerable success, using downward continuations for control. Malahoff and Woollard (1966), working in the low magnetic latitudes of the Hawaiian Archipelago, used the prismatic model method of Vacquier

et al. (1951) with equal success, and supplemented the analysis with two-dimensional model studies.

Both Peters' method and the method of Vacquier et al. assume that the causitive body is polarized by induction in the earth's field. However, whereas the half-slope method is valid only for the vertical component of the magnetic field or for total intensity values in high magnetic latitudes where the horizontal component is negligible, the prismatic model method is useful for total intensity analysis at all angles of magnetic inclination--if the appropriate magnetization vector is used. As shown in Fig. 9, magnetic inclination or dip of 50° to 58° characterizes the area of the Scotia Sea. Consequently, the analytical techniques used for this region must be particularly applicable to intermediate geomagnetic latitudes. Furthermore, since the same anomaly pattern may be explained by various combinations of dimensions, depth, and susceptibility contrast, it is necessary to place limits on the variance of these parameters. In the present study, determination of a first approximation of the depth distribution of anomaly sources was the main objective.

The analytical techniques outlined by Vacquier et al. (1951) were used to determine the following parameters:

1. the approximate depth to the top of the anomalous body,
2. the approximate size and shape of the body, and
3. the probable magnetization contrast (apparent susceptibility contrast or K_A) between the hypothetical geologic body and the surrounding country rock.

Fig. 9. The magnetic inclination in the Scotia Sea for the year 1965, after Oceanographic Office Chart No. 1700 (1965). Contour interval, 2 degrees.

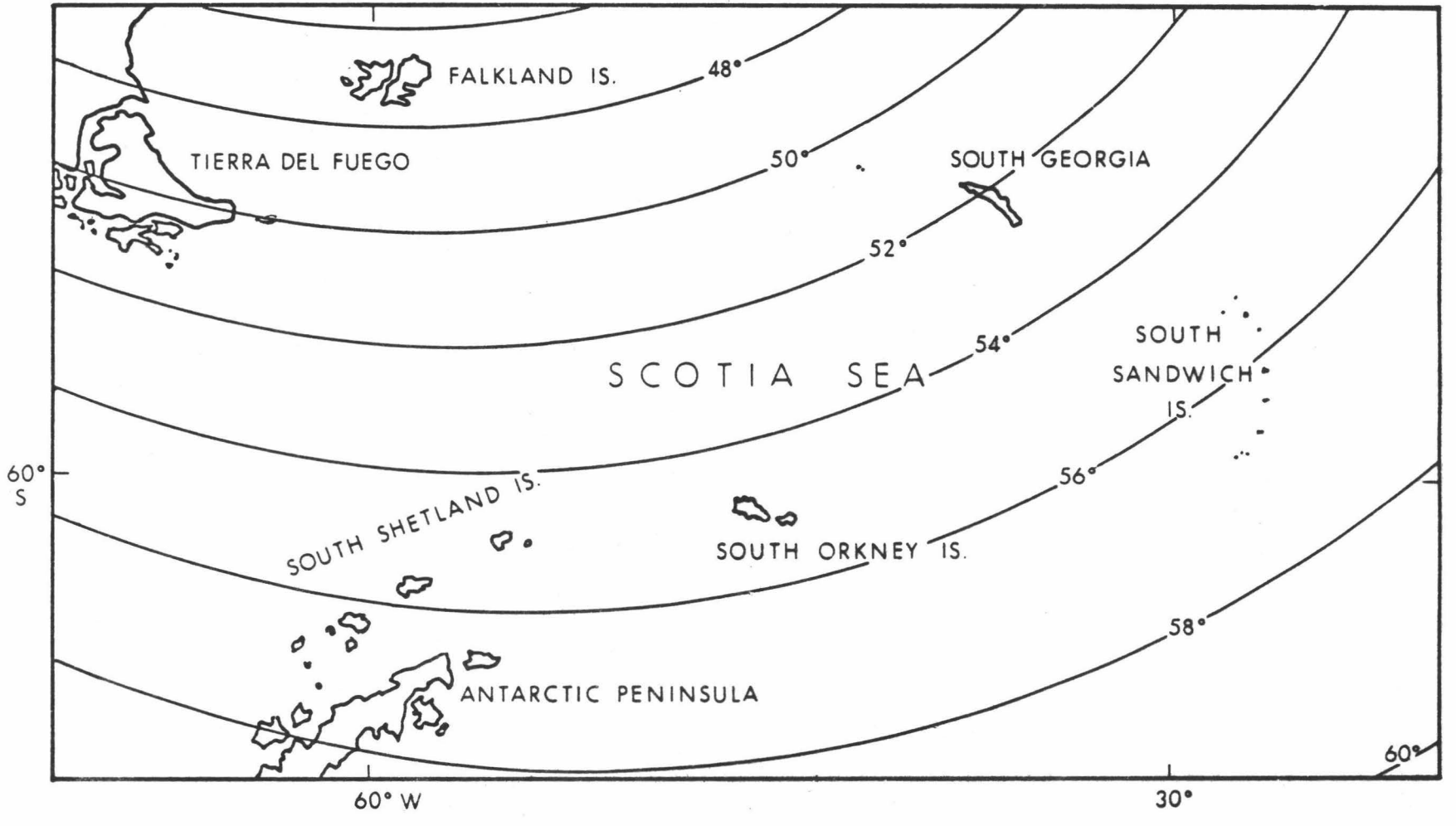
FALKLAND IS.
48°
TIERRA DEL FUEGO
50°
SOUTH GEORGIA
52°
54°
SOUTH
SANDWICH
IS.
SCOTIA SEA
60°
S
SOUTH SHETLAND IS.
56°
SOUTH ORKNEY IS.
58°
ANTARCTIC PENINSULA
60°
60° W
30°

Inherent in these techniques, however, are certain assumptions which are:

1. that the hypothetical body can be approximated by a prismatic cell with vertical side walls, great vertical extent, and a horizontal upper surface not less than one depth-unit below the plane of the map;
2. that the cell is polarized in the direction of the earth's main field;
3. that the apparent magnetic susceptibility is constant throughout the cell and in contrast to the apparent susceptibility of rock surrounding the cell.

Any serious departure from any of the above assumptions will necessarily invalidate the results.

The procedure used to determine the parameters set forth consists in comparing theoretical charts of the total intensity resulting from prismatic cells with variable dimensions (for the proper magnetic inclination), with the actual observed anomalies. In practice, the residual anomaly map of the Scotia Sea (Fig. 6) was examined first and the ELTANIN tracks which ran most nearly perpendicular to the strike of the anomalies were selected. The total intensity values along these tracks were redetermined using a higher data density to facilitate plotting the profiles. The regional gradient was next removed and a residual profile constructed. Most of the short wavelength residual anomalies compared favorably with the theoretical anomaly for the 1 x 6 model of Vacquier et al. (1951). However, longer wavelength anomalies appeared to distort the superimposed shorter wavelengths

and in turn to be somewhat masked by them. A new regional gradient was then drawn through the residual profile so that each short wavelength anomaly conformed rigorously to the theoretical shape. This operation, in effect, visually filtered the long wavelengths in order to separate the various superimposed anomalies. The new residual was then plotted and analyzed. This procedure was found to give fairly consistent depth estimates. Upon examining the new or second regional it was found to consist either of intermediate or of long wavelength anomalies, or a combination of both, which also closely conformed to the theoretical shape. Depth estimates performed on these longer wavelength anomalies gave much greater but still geologically reasonable depths. At this point, in order to test the above method, a series of theoretical overlapping profiles was constructed (Fig. 10). These represented anomalies from variously spaced prismatic cells corresponding to the theoretical 1 x 6 model of Vacquier and others (1951). This was done both for a series of normally magnetized hypothetical cells and for a series of alternating normally and reversely magnetized cells. The profiles comprising each series were then algebraically added as shown in Fig. 10.

Although depth estimates performed on all the waveforms in Fig. 10 are accurate to within 25% of the theoretical depth, the apparent susceptibilities (K_A) are distorted and there is a possibility of mistakenly identifying composite anomalies as long wavelength anomalies resulting from deep (non-existent) structures. Furthermore, it should be mentioned that reversals of magnetization were not observed in the

Fig. 10. Hypothetical magnetic anomalies for an inclination of 60° as caused by variously spaced prisms conforming to the 1 x 6 model of Vacquier et al. (1951). The upper profile represents the effect of normally magnetized prisms; the lower profile, that of alternately normal (N) and reversely (R) magnetized prisms.

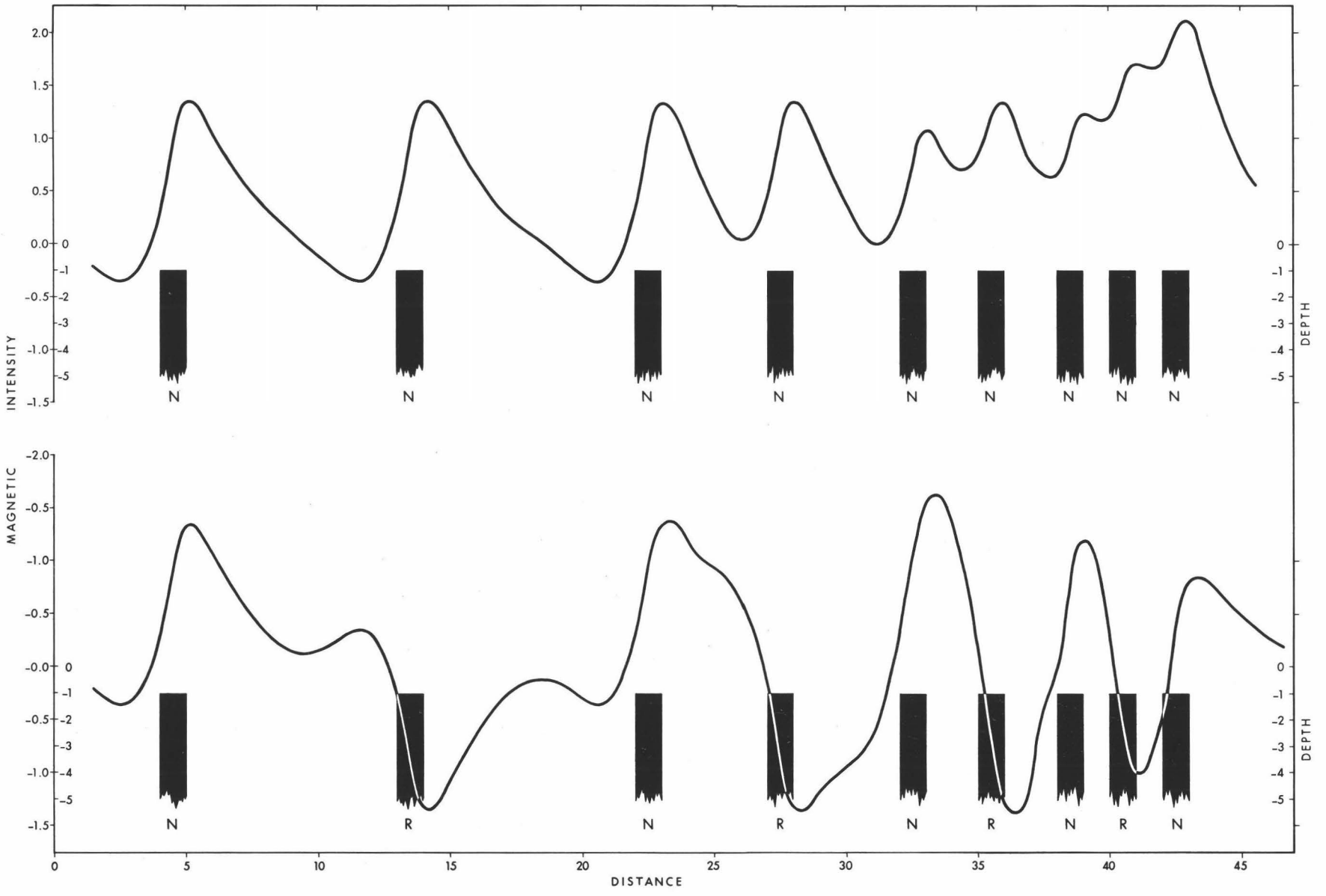
INTENSITY
MAGNETIC
DEPTH
DISTANCE
N
R

profiles examined for detailed analysis from the Scotia Sea. The reason for this apparent absence of reversals in magnetic field is not known, but if reversals in magnetization do not occur here, this would suggest an absence of sea-floor spreading as deduced by Vine and Matthews (1963) from reversals of the earth's magnetic field. However, any errors introduced by mistakenly identifying a reversely magnetized anomaly as a normally magnetized one would not seriously affect the resulting depth estimate.

Depth estimates were made using the horizontal extent of the steepest gradient in conjunction with the Vacquier G index. This procedure generally provides an estimate of maximum depth of origin.

The apparent susceptibility contrast (K_A) between the source of the anomalies and the surrounding rock was estimated using the formula (Vacquier et al., 1951)

$$K_A = \frac{\Delta T_m}{T \cdot \Delta T_c}$$

where ΔT_m is the maximum amplitude of the actual anomaly (in gammas), ΔT_c is the maximum theoretical amplitude from the appropriate Vacquier model, and T is the average total intensity (the regional field in gammas) for the area of investigation.

The results of the above analysis for the western and central Scotia Sea are summarized and discussed in the following section.

Estimated Depth to Magnetic Basement

Depth estimates were made using the approach outlined above on

anomalies over the western and central Scotia Sea. Care was taken to use data from only those tracks which were oriented normal to the residual trends as shown in Fig. 6. Care was also taken to choose tracks which were least affected by changes in course and speed. Low amplitude, short wavelength anomalies which could result from topographic relief were not considered in making the analysis. The results of this analysis are summarized in Table I. The data given included the time of crossing, the geographic position of the anomaly, estimated depth to the top of the source, water depth, depth of the source below the sea floor, and magnetization contrast. The location of depth estimates are plotted in Fig. 11 together with the positions of the seismic refraction lines of Ewing and Ewing (1959).

From Table I it is apparent that the majority of the anomalies examined from the western area originate from sources averaging 5 km below sea level (1-1/2 km below the sea floor). The depth of this layer appears to be in agreement with the depth to the 6.5 km/sec layer as determined by Ewing and Ewing. Evidence is also present which suggests deeper levels of origin. The 14-km average source-depth seems reasonable when compared with the refraction depth in this area of 13 km to the Mohorovicic (M) discontinuity (Ewing and Ewing, 1959). Possibly another level averaging 25-1/2 km below sea level might be related to the curie temperature isotherm.

To the east, however, in the central Scotia Sea, depth estimates indicate that the anomaly source levels are slightly deeper. The shallow source depths average 5-1/2 km below sea level, with the two

TABLE I. MAGNETIC DEPTH ESTIMATES IN THE SCOTIA SEA

Date	GCT	Lat., S	Long., W	Est. Depth, km	Water Depth, km	Depth Below Sea Floor, km	K_A, cgs units
			A. Western Scotia Sea				
			Shallow Sources				
22 July 62	0335	56° 30.5'	61° 50.5'	4	4	0	0.33×10^{-3}*
	0410	56° 37.0'	61° 52.0'	4	4	0	0.33×10^{-3}*
	0550	56° 54.1'	61° 56.5'	5	4	1	2.4×10^{-3}
	0705	57° 06.9'	61° 58.9'	4-1/2	3-1/2	1	1.7×10^{-3}
	1015	57° 33.5'	62° 05.0'	4-1/2	4	1/2	0.80×10^{-3}*
	1125	57° 43.7'	62° 06.1'	5	3	2	1.2×10^{-3}
	1155	57° 48.8'	62° 06.4'	3-1/2	2-1/2	1	2.3×10^{-3}
	1250	57° 57.1'	62° 10.0'	3-1/2	3	1/2	0.64×10^{-3}*
	1335	58° 04.5'	62° 11.9'	3	3	0	0.64×10^{-3}*
30 July 62	0840	58° 16.4'	62° 53.0'	7	4	3	1.7×10^{-3}
	1005	58° 32.1'	62° 55.0'	6	3-1/2	2-1/2	1.7×10^{-3}
11 Dec. 62	0230	56° 36.6'	60° 24.2'	4	3-1/2	1/2	3.3×10^{-3}
	0335	56° 27.0'	60° 26.9'	4	4	0	3.2×10^{-3}
	0535	56° 09.1'	60° 31.0'	5	4	1	1.7×10^{-3}
	0625	56° 02.0'	60° 33.0'	4-1/2	4	1/2	2.4×10^{-3}
	0705	55° 56.2'	60° 34.8'	5-1/2	4	1-1/2	4.6×10^{-3}

TABLE I. (Continued) MAGNETIC DEPTH ESTIMATES
IN THE SCOTIA SEA

Date	GCT	Lat., S	Long., W	Est. Depth, km	Water Depth, km	Depth Below Sea Floor, km	K_A, cgs units
			A. Western Scotia Sea				
			Shallow Sources (Continued)				
11 Dec. 62	0830	55° 43.8'	60° 37.8'	6	4	2	2.3×10^{-3}
(Continued)	0930	55° 35.2'	60° 39.0'	4-1/2	4	1/2	2.6×10^{-3}
	1025	55° 27.1'	60° 41.0'	6-1/2	4	2-1/2	2.9×10^{-3}
8 June 63	2150	58° 17.5'	61° 52.2'	3-1/2	3	1/2	0.81×10^{-3}*
9 June 63	0030	58° 01.9'	61° 36.9'	5-1/2	3	2-1/2	1.2×10^{-3}
	0105	57° 58.3'	61° 33.0'	7-1/2	3	4-1/2	5.4×10^{-3}
	0325	57° 44.5'	61° 22.0'	4-1/2	4	1/2	0.60×10^{-3}*
	0455	57° 35.5'	61° 10.9'	5-1/2	3-1/2	2	0.82×10^{-3}*
		Average, 24 anomalies		5	3-1/2	1-1/2	1.9×10^{-3}
			Intermediate Sources				
22 July 62	0230	56° 18.5'	61° 47.9'	9	4	5	3.5×10^{-3}
	0940	57° 28.7'	62° 03.1'	13	4	9	0.90×10^{-3}
	1230	57° 54.3'	62° 09.0'	14	3-1/2	10-1/2	2.6×10^{-3}

TABLE I. (Continued) MAGNETIC DEPTH ESTIMATES
IN THE SCOTIA SEA

Date	GCT	Lat., S	Long., W	Est. Depth, km	Water Depth, km	Depth Below Sea Floor, km	K_A, cgs units
			A. Western Scotia Sea				
			Intermediate Sources (Continued)				
30 July 62	0530	57° 42.0'	62° 49.2'	13	3-1/2	9-1/2	2.5×10^{-3}
	0755	58° 08.1'	62° 52.0'	15	3-1/2	11-1/2	3.1×10^{-3}
	1135	58° 49.6'	62° 56.4'	11-1/2	3-1/2	8	8.0×10^{-3}
11 Dec. 62	0255	56° 32.8'	60° 25.1'	18	3-1/2	14-1/2	2.3×10^{-3}
	0440	56° 17.0'	60° 29.1'	18	4-1/2	13-1/2	3.8×10^{-3}
9 June 63	0240	57° 54.9'	61° 30.0'	17	3-1/2	13-1/2	4.3×10^{-3}
		Average, 9 anomalies		14	3-1/2	10-1/2	3.4×10^{-3}
			Deep Sources				
22 July 62	0535	56° 51.9'	61° 55.5'	33	3-1/2	29-1/2	3.6×10^{-3}
30 July 62	1000	58° 31.0'	62° 55.0'	22	3-1/2	18-1/2	2.0×10^{-3}

TABLE I. (Continued) MAGNETIC DEPTH ESTIMATES
IN THE SCOTIA SEA

Date	GCT	Lat., S	Long., W	Est. Depth, km	Water Depth, km	Depth Below Sea Floor, km	K_A, cgs units
			A. Western Scotia Sea				
			Deep Sources (Continued)				
11 Dec. 62	0845	55° 41.7'	60° 37.3'	21	4	17	1.0×10^{-3}
		Average, 3 anomalies		25-1/2	3-1/2	21-1/2	2.2×10^{-3}
			Summary				
		* 8 Low K_A Shallow Sources		4	3-1/2	1/2	0.62×10^{-3}
		16 High K_A Shallow Sources		5	3-1/2	1-1/2	2.5×10^{-3}
		9 Intermediate Sources		14	3-1/2	10-1/2	3.4×10^{-3}
		3 Deep Sources		25-1/2	3-1/2	21-1/2	2.2×10^{-3}
			B. Central Scotia Sea				
			Shallow Sources				
11 Mar. 63	0605	57° 37.8'	45° 36.2'	4-1/2	3	1-1/2	0.80×10^{-3} *

TABLE I. (Continued) MAGNETIC DEPTH ESTIMATES
IN THE SCOTIA SEA

Date	GCT	Lat., S	Long., W	Est. Depth, km	Water Depth, km	Depth Below Sea Floor, km	K_A, cgs units
			B. Central Scotia Sea				
			Shallow Sources (Continued)				
11 Mar. 63	0715	57° 26.4'	45° 41.0'	3-1/2	3	1/2	0.46×10^{-3}*
(Continued)	0815	57° 17.5'	45° 45.0'	8	3	5	1.0×10^{-3}
	0915	57° 07.8'	45° 49.0'	3-1/2	3-1/2	0	2.6×10^{-3}
	1000	57° 00.9'	45° 52.0'	5-1/2	3-1/2	2	1.6×10^{-3}
	1035	56° 55.1'	45° 54.1'	3-1/2	3-1/2	0	0.93×10^{-3}*
	1125	56° 47.2'	45° 57.9'	5	3-1/2	1-1/2	1.0×10^{-3}
	1325	56° 28.2'	46° 06.2'	4	4	0	1.5×10^{-3}
	1420	56° 20.0'	46° 10.0'	4	4	0	0.59×10^{-3}*
	1605	56° 03.8'	46° 15.1'	7	4	3	1.4×10^{-3}
	1810	55° 43.6'	46° 23.0'	7	4	3	2.1×10^{-3}
	1915	55° 34.0'	46° 27.9'	6-1/2	4	2-1/2	1.2×10^{-3}
	2025	55° 24.9'	46° 36.5'	6	3-1/2	2-1/2	4.6×10^{-3}
	2345	54° 58.0'	47° 06.0'	4	?	?	0.44×10^{-3}*
12 Mar. 63	0010	54° 54.4'	47° 09.4'	8	4-1/2	2-1/2	3.0×10^{-3}
	0110	54° 44.2'	47° 18.9'	4	3-1/2	1/2	0.98×10^{-3}*
	0145	54° 38.5'	47° 24.2'	7-1/2	3-1/2	4	5.6×10^{-3}
	0245	54° 28.5'	47° 33.8'	7	3-1/2	3-1/2	1.4×10^{-3}

TABLE I. (Continued) MAGNETIC DEPTH ESTIMATES
IN THE SCOTIA SEA

Date	GCT	Lat., S	Long., W	Est. Depth, km	Water Depth, km	Depth Below Sea Floor, km	K_A, cgs units
			B. Central Scotia Sea				
			Shallow Sources (Continued)				
12 Mar. 63 (Continued)	0330	54° 21.2'	47° 40.8'	3-1/2	3-1/2	0	0.54×10^{-3}*
	0350	54° 18.0'	47° 43.9'	7-1/2	3-1/2	4	4.9×10^{-3}
	0430	54° 11.8'	47° 50.0'	4-1/2	4	1/2	0.56×10^{-3}*
	0510	54° 05.1'	47° 56.4'	5	4	1	3.2×10^{-3}
		Average, 22 anomalies		5-1/2	3-1/2	2	1.8×10^{-3}
			Intermediate Sources				
11 Mar. 63	0235	58° 09.9'	45° 22.5'	13	3	10	1.7×10^{-3}
	0355	57° 58.0'	45° 27.8'	18	2-1/2	15-1/2	1.0×10^{-3}
	0720	57° 26.0'	45° 41.1'	18-1/2	3	15-1/2	0.69×10^{-3}
	0855	57° 10.7'	45° 47.4'	11	3-1/2	7-1/2	1.2×10^{-3}
	1130	56° 46.4'	45° 58.0'	14	3-1/2	10-1/2	1.3×10^{-3}
	1355	56° 24.0'	46° 08.9'	18-1/2	4	14-1/2	3.4×10^{-3}
		Average, 6 anomalies		15-1/2	3-1/2	12	1.5×10^{-3}

TABLE I. (Continued) MAGNETIC DEPTH ESTIMATES
IN THE SCOTIA SEA

Date	GCT	Lat., S	Long., W	Est. Depth, km	Water Depth, km	Depth Below Sea Floor, km	K_A, cgs units
			B. Central Scotia Sea				
			Deep Source				
11 Mar. 63	1530	56° 08.0'	46° 13.5'	37-1/2	3-1/2	34	1.3×10^{-3}
		(1 anomaly observed)					
			Summary				
		* 8 Low K_A Shallow Sources		4	3-1/2	1/2	0.66×10^{-3}
		14 High K_A Shallow Sources		6	3-1/2	2-1/2	2.5×10^{-3}
		6 Intermediate Sources		15-1/2	3-1/2	12	1.5×10^{-3}
		1 Deep Source		37-1/2	3-1/2	34	1.3×10^{-3}

Fig. 11. Location of magnetic depth estimates and of seismic refraction lines of Ewing and Ewing (1959).

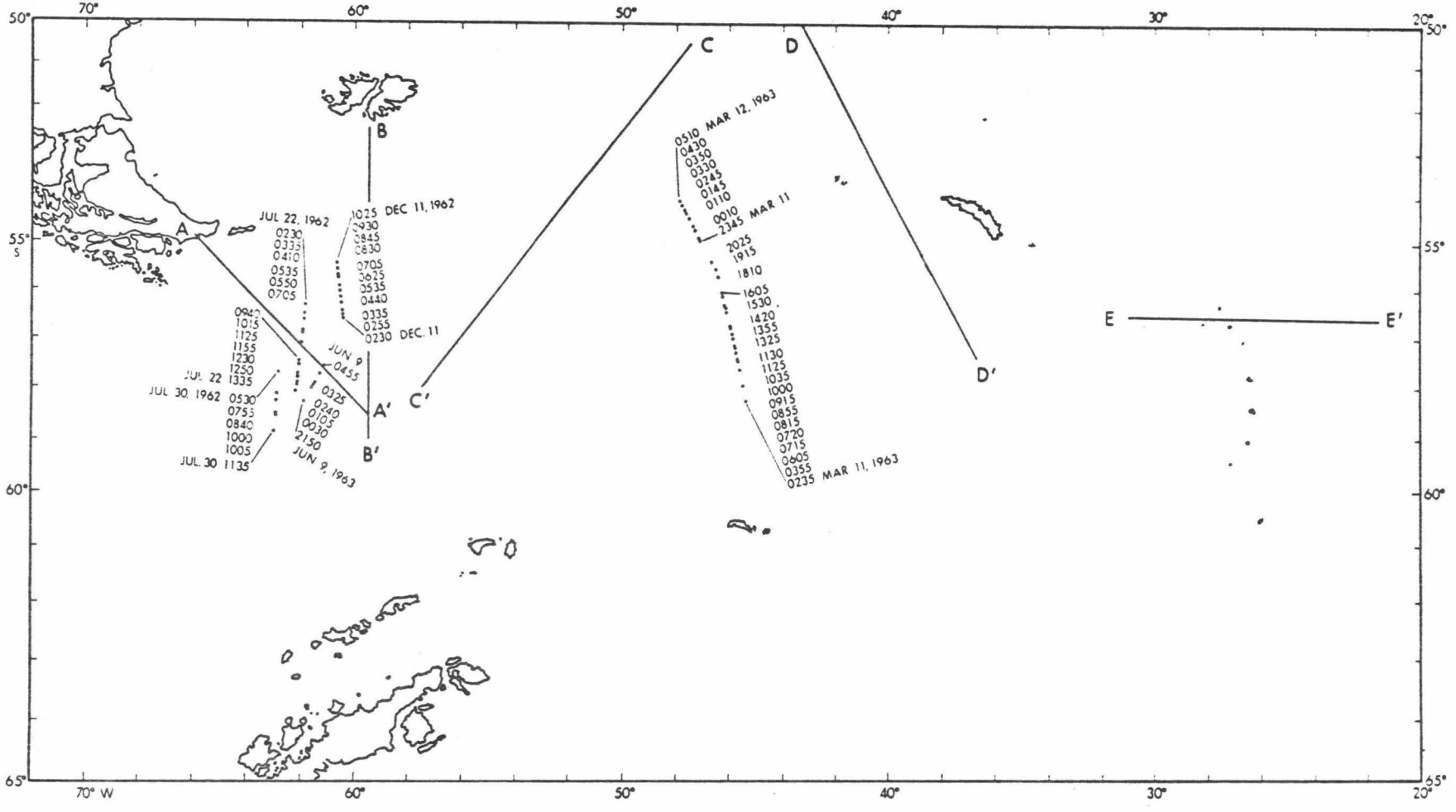
70°
60°
50°
40°
30°
20°
50°
55°
S
60°
65°
70° W
A
A'
B
B'
C
C'
D
D'
E
E'
JUL 22, 1962
0230
0335
0410
0535
0550
0705
0940
1015
1125
1155
1230
1250
JUL 22
1335
JUL 30, 1962
0530
0755
0840
1000
1005
JUL. 30 1135
1025 DEC 11, 1962
0930
0845
0830
0705
0625
0535
0440
0335
0255
0230 DEC. 11
JUN 9
0455
0325
0240
0105
0030
2150
JUN 9, 1963
0510 MAR 12, 1963
0430
0350
0330
0245
0145
0110
0010
2345 MAR 11
2025
1915
1810
1605
1530
1420
1355
1325
1130
1125
1035
1000
0915
0855
0815
0720
0715
0605
0355
0235 MAR 11, 1963

deeper sources, one at about 15-1/2 kilometers and the other at 37-1/2 kilometers below sea level (Table I).

It should be noted that although the depth estimates obtained from the long wavelength anomalies could represent sources near the M discontinuity or possibly the curie temperature isotherm, the same anomalies could also possibly result from a lateral, near-surface (sea floor) distribution of magnetic materials, i.e., a gradual variation in magnetization contrast with horizontal extent. However, this would require that the surface distribution of the variation in magnetization fall into the two groups observed. This seems unlikely. The alternative to this would be an error in identifying superimposed anomalies--as previously discussed.

Possible Origin of the Magnetic Anomalies

Definitive remarks on the genesis of the structure causing the magnetic anomalies over the Scotia Sea would be at best only speculative at this time. However, considering the amount of magnetic data in existence, and the availability of supporting seismic refraction measurements, a working hypothesis can be formulated regarding the geologic origin of the structure.

Magnetization contrasts in the West Scotia Basin were estimated from the magnetic anomalies given in Table I, using Vacquier's method as previously described. The values obtained for the anomalies of shallow origin range between 0.33×10^{-3} and 4.6×10^{-3} cgs units, averaging 1.9×10^{-3} cgs units. Depths to the top of the sources of these anomalies range between 3 and 7-1/2 km below sea level, averaging

5 km below sea level or approximately 1-1/2 km below the ocean floor. If the anomalies are grouped and averaged with regard to their relative values of K_A, it is seen that the anomalies with relatively low K_A (averaging 0.62×10^{-3} cgs units) originate at approximately 1/2 km below the sea floor whereas those with relatively high K_A (averaging 2.5×10^{-3} cgs units) have their depths of origin 1-1/2 km below the ocean floor. In addition, the anomalies of intermediate depths of origin have magnetization contrasts ranging between 0.9×10^{-3} and 8.0×10^{-3} cgs units, or an average of 3.4×10^{-3} cgs units. Source depths for these anomalies range between 9 and 18 km below sea level and, as stated earlier, average 14 km below sea level, or near the M discontinuity. Finally, the deep sources exhibit an average magnetization contrast of 2.2×10^{-3} cgs units for an average depth of origin of 25-1/2 kilometers.

The apparent increase in magnetization contrast with depth to the level of the M discontinuity, although geologically reasonable, may only be fortuitous. This phenomenon, however, should be investigated further and examined more critically in order to determine any definite correlation.

In the central Scotia Sea, average source depths appear to occur at slightly deeper levels, as previously shown; however, magnetization contrasts for the shallow and deep anomalies (Table I) appear in extremely close agreement with those from the western Scotia Sea. The K_A of the intermediate anomalies, however, appears significantly lower in the central Scotia Sea.

As in the West Scotia Basin, the shallow anomalies in the central area may be grouped according to their relative magnetization contrasts. Anomalies with relatively low K_A (averaging 0.66×10^{-3} cgs units) originate about 1/2 km below the sea floor while those with relatively high K_A (averaging 2.5×10^{-3} cgs units) originate at 2 km below the sea floor. Anomalies of intermediate depths of origin, however, have magnetization contrasts averaging 1.5×10^{-3} cgs units (compared with 3.4×10^{-3} cgs units for the western area) for an average depth of origin of 15-1/2 km below sea level.

Whether this decrease in K_A and increase in depth to the east indicates a decreasing contrast in the physical properties of the material near the M discontinuity is conjectural. The significance of this observation remains to be established. It should be pointed out here that the average of the observed K_A of the deeper layers may be too high. This may simply reflect a bias stemming from the inability to recognize small amplitude anomalies of long wavelength.

Nagata (1961) has shown "the magnetic susceptibility of rocks in weak magnetic fields such as that of the earth depends on the kind and abundance of ferromagnetic mineral grains and their size in a complicated manner." Furthermore, he states that "the magnitude of the natural remanent magnetization [J_r] of igneous rocks is almost invariably greater than the induced magnetization in the present geomagnetic field." In support of this, Vogt and Ostenso (1966) demonstrate that oceanic basalts have uniformly low susceptibilities and high intensities of remanent magnetization (the effect of which is an order of magnitude

greater), and conclude that apparent susceptibility is primarily a function of J_r, irrespective of whether the inducing field is reinforcing or opposing.

From this it would appear that, without knowing the susceptibility (k), or the value or direction of J_r, little confidence can be placed in the estimate of rock type as determined from magnetic anomalies. Fortunately, however, many recent determinations have been made of k and J_r values for rocks from oceanic areas (Table II). From these data one might speculate on the type of lithology present in the area under investigation.

Since it is probable that there is a considerable J_r, it would be reasonable--on the basis of magnetization contrasts (K_A in Table I) and data from Table II--to visualize the source of the very shallow anomalies (low K_A) in the western and central Scotia Sea as hydrothermally altered intrusions of basalt into a sedimentary sequence or, more simply, as topographic relief of a hydrothermally altered basalt basement blanketed by sediments. Likewise, the slightly deeper (less shallow) anomalies could be explained in a similar manner as being caused by intrusions of unaltered (fresh) basalt (having a higher K_A) into or through an older hydrothermally altered basaltic layer in the vicinity of rift zones, or even by alternating vertical zones of low-grade hydrothermally metamorphosed peridotite and basalt.

Luyendyk and Melson (1967) point out that low-grade hydrothermal alteration can significantly decrease the magnetic properties of basalts and can produce the opposite effect on peridotites. They

TABLE II. MAGNETIC PROPERTIES OF ROCKS FROM THE ATLANTIC AND PACIFIC OCEANS

Description	k, emu/cm^3 x 10^{-3}	J_r, emu/cm^3 x 10^{-3}	Q
Aphanitic basalt but with some crystals visible, including olivine. Chocolate colored, weathered, 5% vesicles (some tabular), 3% white amygdules*	0.63	1.69	5.7
Fine-grained basalt with a few small vesicles*	0.26	7.29	58.4
Fine-grained basalt with 3% vesicles, some with light brown linings*	0.26	7.79	63.5
Dense basalt with a few small vesicles*	0.40	11.50	60.0
Fine-grained basalt with a few crystals visible, 8% vesicles 0.1 to 1 mm in diameter*	0.16	9.40	121.0
Fine-grained basalt with a few crystals visible and a few vesicles 0.1 mm to 0.5 mm in diameter*	0.87	4.62	11.1
Fine-grained basalt with 10% olivine phenocrysts 1/2 to 3 mm in diameter and 2% vesicles 0.1 to 0.5 mm in diameter*	0.15	6.80	95.7

TABLE II. (Continued) MAGNETIC PROPERTIES OF ROCKS
FROM THE ATLANTIC AND PACIFIC OCEANS

Description	k, emu/cm^3 x 10^{-3}	J_r, emu/cm^3 x 10^{-3}	Q
Fine-grained basalt*	0.30	2.32	16.5
Brittle, glass-sheathed fragments of basalts*	0.06	0.76	27.5
Basalt with glass sheath*	0.20	0.56	5.9
Median value*	0.3	5.0	48
Median value of 43 samples from abyssal hills on the floor of the North Atlantic Ocean from Vogt and Ostenso (1966) after Matthews (1961)	0.5	4.4	20.0
Median value of 97 samples from the Atlantic and Pacific oceans from Vogt and Ostenso (1966) after Ade-Hall (1964)	0.5	5.0	18.0
Median value of unknown number of samples from the Mendocino escarpment from Vogt and Ostenso (1966) after Bullard and Mason (1963)	1.8	17.7	20.0
Median value of 23 samples from Mohole test site EM7 (Guadalupe site) from Vogt and Ostenso (1966) after Cox and Doell (1962)	0.3	5.0	40.0

TABLE II. (Continued) MAGNETIC PROPERTIES OF ROCKS
FROM THE ATLANTIC AND PACIFIC OCEANS

Description	k, emu/cm^3 x 10^{-3}	J_r, emu/cm^3 x 10^{-3}	Q
Fresh, medium-grained basalt with about 3 per cent by volume equidimensional titanomagnetic crystals**	1.57 1.88	3.63 3.60	4.62 3.84
Fresh, coarse-grained olivine basalt, with approximately 4 per cent by volume equidimensional crystals of titanomagnetite. This sample in view of its unusually coarse grain size, may be an intrusive (dike or sill) rock**	2.69 2.86 2.98	4.74 4.67 5.01	3.52 3.26 3.36
"Quenched", fine-grained olivine basalt with abundant interstitial glass rich in titanomagnetite (?) and ilmeno-hematite in extremely small platy crystals arranged in a rectangular grid-like manner**	0.81 0.75 0.64	11.29 8.26 9.55	27.87 21.95 29.85
Brecciated basalt, considerable secondary saponite. Probably a fault breccia. Titanomagnetite altered to sphene and ilmeno-hematite**	0.09 0.11 0.32 0.22	0.25 0.40 0.64 0.36	5.32 7.32 4.03 3.23
Fine-grained, saponite-rich, brecciated basalt. Oxides altered to goethite and ilmeno-hematite (?)**	0.08 0.09 0.13	0.05 0.06 0.13	1.37 1.94 2.02

TABLE II. (Continued) MAGNETIC PROPERTIES OF ROCKS
FROM THE ATLANTIC AND PACIFIC OCEANS

Description	k, emu/cm^3 x 10^{-3}	J_r, emu/cm^3 x 10^{-3}	Q
Basalt fragment from tectonic breccia. Considerable secondary saponite mainly replacing olivine. Interstitial, devitrified glass with abundant platy crystals of titanomagnetite (?)**	1.58 1.85	2.29 2.45	2.90 2.66
Greenstone. Contains albite, actinolite, epidote, chlorite, and sphene in various amounts. Fe-Ti oxides totally replaced by silicates**	0.06	0.01	0.38
Greenstone. Contains albite, actinolite, epidote, chlorite, and sphene in various amounts. Fe-Ti oxides totally replaced by silicates**	0.05	0.005	0.20
Greenstone. Contains albite, actonolite, epidote, chlorite, and sphene in various amounts. Fe-Ti oxides totally replaced by silicates**	0.04	0.002	0.08

*Dredged from the flanks of the Mid-Atlantic Ridge after Vogt and Ostenso (1966).

**Dredged from near the crest of the Mid-Atlantic Ridge after Luyendyk and Melson (1967).

further state that "if a terrain were initially composed of alternate zones of fresh basalts and fresh peridotites, strong anomalies might be expected over the former. If this region then underwent low-grade hydrothermal metamorphism, high anomalies would be expected over the former peridotite zones, and minima over the basalt zones."

The sources of the anomalies with intermediate depths of origin are even more conjectural. Considering their depth of origin (averaging 14 to 15-1/2 km) it would be reasonable to assume that the anomalies indicate variations in the magnetic properties of the mantle. However, as previously discussed, the depth estimates probably indicate the lowest level at which the sources may occur and the possibility does exist that the wrong theoretical model was inadvertently chosen for comparison. Either situation could cause the actual source depths to be shallower than estimated; in which case, the anomalies could be considered to result from intrusions of mantle-like or mantle-derived material into the overlying crustal rock--such as is noted in connection with the Molokai Fracture Zone north of Maui (Furumoto and Woollard, 1965; Malahoff and Woollard, 1966). Extrapolating this further, the anomalies may even be the result of alternate vertical zones of (fresh) basalt and (fresh) peridotite, as suggested by the work of Luyendyk and Melson.

Assuming the estimated depths of the deep sources are correct, it appears most reasonable to visualize the cause of these low amplitude, long wavelength anomalies in terms of varying elevation of the

curie temperature isotherm. Precedence has been established for this interpretation in papers by Vacquier et al. (1951), Nagata (1961), and Sankar-Narayan (1961).

BATHYMETRY OF THE SCOTIA SEA

One of the first bathymetric charts to show the general configuration of the bottom topography of the Scotia Sea was that published by Herdman in 1932. It was based on soundings obtained between 1926 and 1932 by the ships of the DISCOVERY Committee. Maurer and Stocks (1933) and Stocks (1937) also published bathymetric charts of the area based on soundings obtained during the METEOR expedition. Included on these charts are selected soundings from the DISCOVERY cruises and from other sources. In 1948, Herdman revised his original chart to include all bathymetric data available at that time, compiled mainly from the published DISCOVERY and METEOR data but also from hitherto unreported DISCOVERY data. The data were corrected by Herdman using Matthew's (1939) tables for variations in the average vertical sound velocity in sea water. Although other contoured charts of the entire region have been published more recently, notably U. S. Naval Hydrographic Office chart H. O. miscellaneous 15,254-11 (1961) and those in the Soviet Atlas of Antarctica (Atlas Antarktiki, 1966), Herdman's 1948 chart appears to remain the most accurate and realistic effort, especially in areas where depths are not inferred.

In 1961 Heezen and Tharp published a physiographic diagram of the South Atlantic including the Scotia Sea. Although the diagram clearly portrays the regional topography and the complexity of the area, relief is often speculative and quite frequently is based on extrapolation of trends (Heezen and others, 1959). Recently a portion of the Scotia Sea has been contoured in greater detail and with greater

precision. Heezen and Johnson (1965) published a new bathymetric chart of the South Sandwich Trench, coupled with a comprehensive evaluation of discernible topographic features. Careful examination of this work reveals lineations and trends previously not portrayed. Partly for this reason and partly to furnish an updated and more complete bathymetric chart for purposes of comparison with the magnetic charts, the entire Scotia Sea was recontoured by the writer (Fig. 12).

From a review of Fig. 2, it was concluded that bathymetry obtained solely from the ELTANIN cruises was insufficient to construct a contour chart of the Scotia Sea. However, using Herdman's 1948 chart for control in areas where ELTANIN data were limited or lacking, re-contouring became feasible. The ELTANIN bathymetry, based on acoustic depths measured in units of 1/400-second travel time or approximately one fathom (Lamont Geological Observatory, 1963-1965), were uncorrected for variation in the vertical sound velocity (Heezen and others, 1959). By superimposing Herdman's 1948 contours on the plotted ELTANIN soundings, adjusting the contours, and adding more detail, the ELTANIN data were contoured in meters for the west and central Scotia Sea. Following this, metric contours were interpolated and traced from Heezen and Johnson's 1965 chart of the South Sandwich Trench and the two sections were joined to form a complete bathymetric chart of the Scotia Sea.

Examination of Matthew's tables (1939) shows that the corrections applied to the DISCOVERY data were negligible in waters of less than

Fig. 12. Bathymetry of the Scotia Sea. Contour interval, 1000 meters; isobaths are also given at the 500-m and 200-m depths.

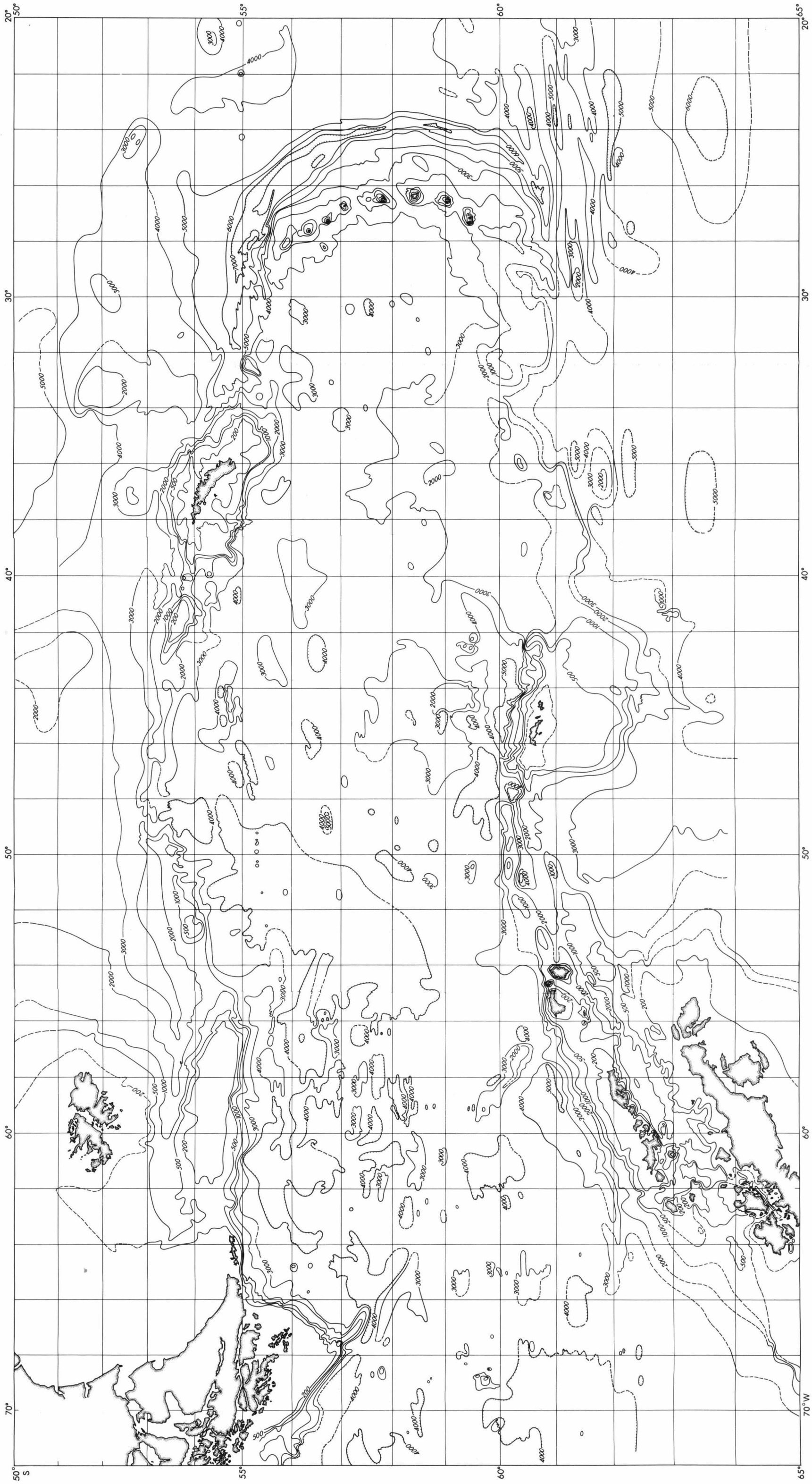
20°
50°
55°
60°
65°
30°
40°
50°
60°
70°
50° S
70° W

3000 meters depth and approximately 2 per cent in waters of greater than 5000 meters depth. Consequently, the amount of shift in the contours is negligible on the scale on which the bathymetric chart is constructed. For this reason the DISCOVERY contours were not changed in combining them with the ELTANIN bathymetry.

Thus, although the resulting chart may lack the desired precision because of the corrections applied to the DISCOVERY data or the lack of corrections to the ELTANIN data, it does appear to portray lineations and regional topographic trends accurately and hence to present a close approximation of the Scotia Sea bathymetry. A chart of higher precision must await release and compilation of all recent bathymetric information, much of it as yet unpublished. Data from the DISCOVERY and METEOR investigations together with data from the sounding tracks reported by Griffiths and others (1965), when combined with the data from the USNS ELTANIN, may make possible construction of a high resolution chart of the area.

In Fig. 12, the contour interval in 1000 meters. Additional isobaths were added at the 200- and 500-m depths to more clearly delineate slopes and shelf areas. The data control is not shown on the chart but may be determined by comparing Fig. 12 with Fig. 2, Herdman's 1948 chart, and Heezen and Johnson's 1965 chart.

The morphology of the Scotia Sea has been previously discussed in detail by several writers, including Herdman in his 1932 report. The most prominent feature of the area is the Scotia Arc consisting of: (1) the north Scotia Ridge originating at Tierra del Fuego and

including Isla de los Estados, Burdwood Bank, Shag Rocks, South Georgia, and Clerke Rocks; (2) the South Sandwich Islands and attendant South Sandwich Trench; and (3) the south Scotia Ridge, terminating against the Antarctic Peninsula and including the South Orkney Islands, Elephant and Clarence Islands Group, and the South Shetland Islands. It should be noted that the Falkland Islands are separated from the north Scotia Ridge by the Falkland Trough north of Burdwood Bank. Of lesser prominence yet of considerable interest are: (1) the unnamed deeps bordering and contiguous to the Scotia Arc in the western and central Scotia Sea; and (2) the North and South Sandwich fracture zones.

From a study of the bathymetric chart of the Scotia Sea (Fig. 12) the following observations have been made:

1. The deeps bordering the inside of the Scotia Arc in the West and Central Scotia basins have the effect of causing the axial region of the Scotia Sea to appear relatively high. Toward the east, as the entire sea floor rises, these deeps gradually terminate northward southwest of South Georgia and southward northeast of the South Orkney Islands.
2. In the eastern Scotia Basin, the sea floor is elevated and becomes progressively so in the direction of the South Sandwich Islands. To this progressive decrease in ocean depth, Heezen and Johnson (1965) drew the analogy of a tilted crustal block uplifted in the vicinity of the island arc.
3. The arcuate ridges behind and concentric to the South Sandwich Islands, shown in Heezen and Tharp's (1961) physiographic

diagram and discussed by Heezen and Johnson, are not as clearly discernible in Fig. 12. This may be the result of the contour interval chosen, but more likely it is due to Heezen and Johnson having had access to more data than did the writer.

4. The South Sandwich Trench abuts against, and appears to be terminated by, the previously mentioned North and South Sandwich fracture zones. As was discussed earlier, in the residual magnetic anomaly chart, the North Sandwich Fracture Zone can be traced considerably farther to the east beyond the area of bathymetric expression. This has the effect of extending the apparent symmetry of the Scotia Sea eastward beyond the South Sandwich Trench.

GEOLOGY AND TECTONICS OF THE SCOTIA SEA

Geology of the Scotia Sea

The general areal geology of the Scotia Arc has been synthesized by Anderson (1965) in his description of the bedrock geology of Antarctica. However, in order to facilitate further discussion, the geology of the area is briefly reviewed here.

The North Scotia Ridge from Burdwood Bank to Shag Rocks and western South Georgia consists mainly of sediments and low grade metasediments with some intercalated tuffs and other volcanic rocks. Localized acidic and basic intrusions are found in eastern South Georgia and Clerke Rocks, with the latter described as "granite cut by basic dikes" (Anderson, 1965).

The South Sandwich Islands are characterized by active volcanism and for the most part consist of basic to intermediate lavas ranging in composition from olivine basalts to andesites. Formerly, sediments or metasediments were thought to crop out on Freezeland Rock (one of the southernmost islands of the South Sandwich Group), but W. Seelig (personal communication) has reported an observation by V. Fuchs that he found no rocks of sedimentary origin there. Gass and others (1963) reported that floating pumice rafts were observed in the vicinity of the South Sandwich Islands. It was suggested that the pumice originated from an explosive eruption of a seamount on the northwestward continuation of the island arc, on the basis of a nearly contemporaneous earthquake with an epicenter located at 55.9°S and 27.9°W. The pumice was described as rhyolitic or rhyodacitic in composition and, if the source is correctly located, represents the most acidic rocks so

far described from the area.

The South Scotia Ridge is characterized by a greater variation in lithology than is true of the northern ridge. The rock types range from graywackes and schists cut by dikes of olivine dolerite in the South Orkney Islands (toward the eastern end of the South Scotia Ridge) to a conglomeration of acidic and basic extrusives and intrusive overlying and intersecting a varied sedimentary and metasedimentary sequence in the South Shetland Islands (at the western extremity of the ridge). An ultrabasic mass comprised of dunite-serpentinite, largely altered to serpentine schist, is reported (Matthews, 1959) to underlie the schists of Gibbs Island within the Elephant and Clarence Islands Group.

In general, the rocks of both the North and South Scotia ridges consist predominately of volcanic-derived sediments (graywackes and mudstones intercalated with tuffs) and are considered by some investigators of the Scotia Sea as typical of a eugeosynclinal environment of deposition. Frequently, the rocks are altered to slates and schists by low-rank regional metamorphism. Also in association are extrusive and intrusive igneous rocks, usually acid to intermediate in composition. The above lithologies together with the rock suites from the North Scotia Ridge are referred to by many writers as being continental rather than oceanic, and as having Andean affinities. Little information is available about the ocean floor in the Scotia Sea. Limited dredgings and some of the bottom photographs studied by Goodell (undated ms.) indicate that the surface of Sars Bank in the West

Scotia Basin "is often pebbly with basalt" and that "outcrops of what appear to be jointed lava flows" occur at 3100 fathoms on the walls of the South Sandwich Trench. Although dredging and bottom photography presently furnish the only direct means of observing the Scotia Sea lithologies within the deep water, it is important to be aware that ice-rafted erratic pebbles, cobbles, and boulders may be superimposed on the primary sediment type (Goodell, undated ms.).

The hypothetical stratigraphic succession and geologic history of the region determined from Adie (1962) and Ford (1964) is shown in Table III. Although the correlations are only tenuous, the chart does furnish theoretical guidelines to be verified or refuted by the accumulated geological and geophysical data.

The structural elements of the region also provide a basis for considerable speculation. Like the lithologies, they appear to have Andean affinities. In general, the regional structure is dominated by fold belts or a succession of fold belts paralleling the axes of the North and South Scotia ridges and consequently the structure of Tierra del Fuego and the Antarctic Peninsula also. Ford (1964) in his review of Antarctic geology presents two interpretations: one after Hamilton (1963) which assigns a Cretaceous age to the folding, and the other after Fairbridge (1952), which dates the folds as Mesozoic and Tertiary.

Structure from Seismic Refraction and Reflection Measurements

Seismic refraction investigations in the Scotia Sea have been reported by Ewing and Ewing (1959). The results of these

TABLE III. GEOLOGIC CORRELATION IN THE SCOTIA ARC (AFTER ADIE, 1962)

Geologic Age	Shag Rocks	South Georgia Island	Clerke Rocks	South Sandwich Islands	South Orkney Islands	South Shetland Islands			
						Elephant & Clarence Islands	King George Island	Deception Island	Livingston Island
Recent		Raised beaches		Andesite-dacite volcanic group (active volcanoes)	Raised beaches; Wave-cut platforms		Raised beaches	Post-Caldera Series: Whalers Bay Group; Pendulum Cove Group; Neptunes Bellows Group	Raised beaches; Wave-cut platforms
Pleistocene		(Glaciation)			(Glaciation)		Penguin Island Group; (Glaciation)		(Glaciation)
Pliocene							Pecten Conglomerate; Point Hennequin Group	Pre-Caldera Series: Port Foster Group	
Miocene		Basic dikes	Basic dikes				Filides Peninsula Group		Younger volcanic Group
Oligocene									
Eocene		Andean Intrusive Suite	Andean Intrusive Suite (granite)				Andean Intrusive Suite		Andean Intrusive Suite
U. Cretaceous		Dikes; Interbedded sediments and spilites of Annenkov Island (marine sediments) and the south coast			Conglomerates				
L. Cretaceous									
U. Jurassic					Diabase dikes		Upper Jurassic Volcanic Group		Older volcanic Group: Renier Point lavas; Mount Bowles agglomerate
M. Jurassic									
Triassic		Marine sediments			Derived Series				
Carboniferous(?)	Graywackes	Marine sediments	Graywackes (known only from erratics)		Graywacke-shale Series				Miers Point Series
Lower Paleozoic									
Precambrian	Schists(?)	Basement Complex			Basement Complex: Moe Island Series; Amphibolite Series; Marble Series	Basement Complex: Phyllites; Schists	Basement Complex		False Bay schists

investigations (Fig. 13) indicate a very thick, low velocity section for the North Scotia Ridge south of the Falkland Trough. Farther to the south, near the axial region of the Scotia Sea in the West Scotia Basin, the crust appears to be of normal oceanic type. To the east, in the shallower parts of the Scotia Sea (East Scotia Basin), the structure appears to differ from both continental and oceanic types. It is problematical that either an intermediate layer is present here between the normal crustal layer and the mantle, or else that a velocity gradient is causing the velocity to reach 7.5 km/sec near the M discontinuity (Ewing and Ewing, 1959). Consequently, resemblance in structure was noted between the shallow parts of the Caribbean and those of the East Scotia Basin, accentuated by the observed similarity between the structure of the Lesser Antilles and that of the South Sandwich Arc where "the crustal layer is arched up along the island arc and deeply depressed under the trench" (Ewing and Ewing, 1959).

Griffiths and others also have reported seismic refraction measurements in the Scotia Sea. Interpretation of the structure of the Bransfield Strait (Fig. 8) was partly based on these data. Here the mantle, represented by high density material (3.27 g/cm^3), is depressed to a depth of more than 30 km under the Antarctic Peninsula. Near the South Shetland Islands a dense (3.1 g/cm^3) high velocity (7.4 km/sec) layer, possibly derived from the mantle, rises to within at least 8 km of sea level and perhaps even to within 5 km of sea level under the islands themselves. This rise of dense material under

Fig. 13. Crustal sections of the Scotia Sea, after Ewing and Ewing (1959).

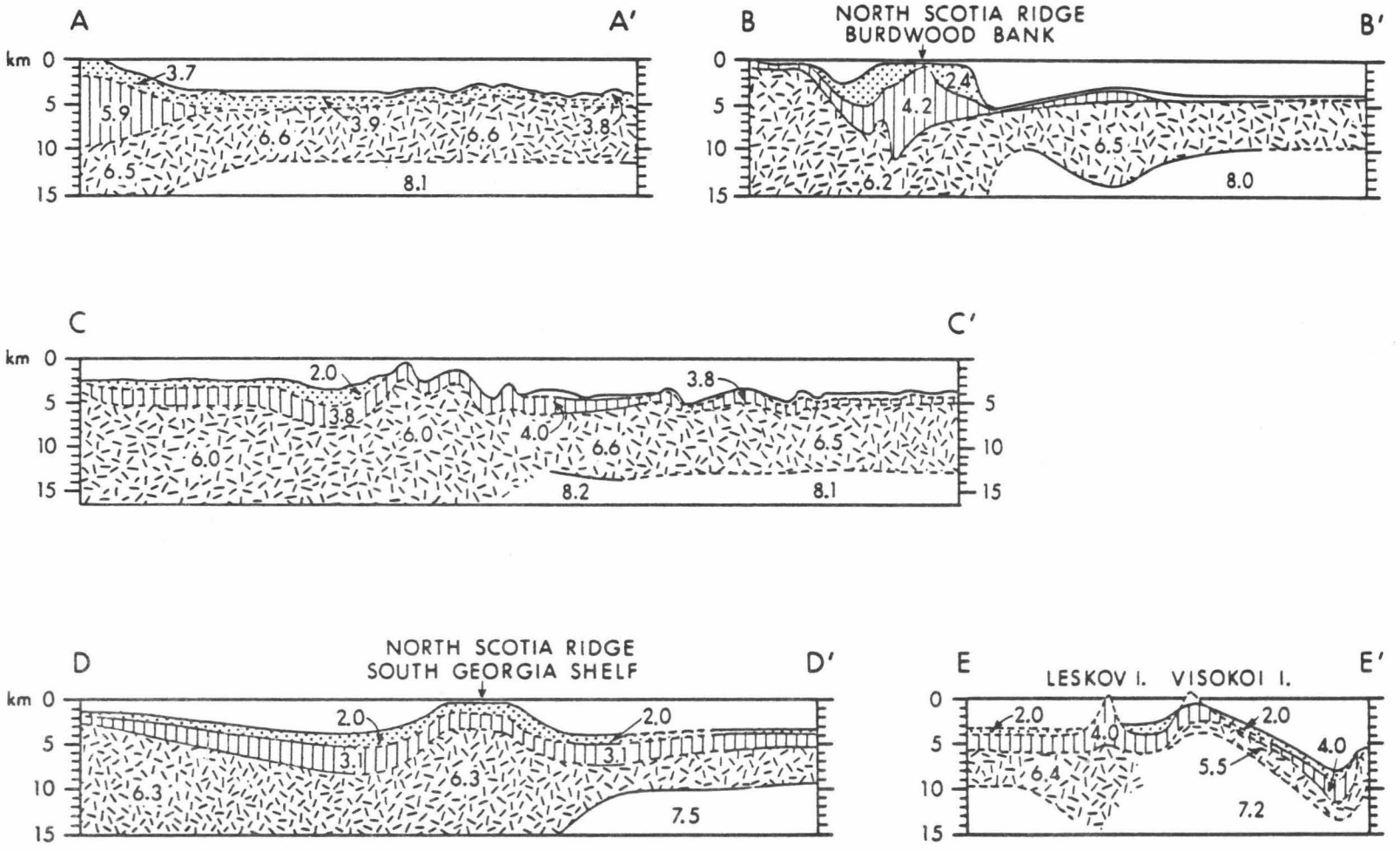
A
A'
km 0
5
10
15
3.7
5.9
6.6
3.9
6.6
3.8
6.5
8.1
B
NORTH SCOTIA RIDGE
BURDWOOD BANK
B'
0
5
10
15
2.4
4.2
6.5
6.2
8.0
C
C'
km 0
5
10
15
2.0
3.8
3.8
6.0
4.0
6.6
6.5
6.0
8.2
8.1
D
NORTH SCOTIA RIDGE
SOUTH GEORGIA SHELF
D'
km 0
5
10
15
2.0
2.0
3.1
3.1
6.3
6.3
7.5
E
LESKOV I.
VISOKOI I.
E'
0
5
10
15
2.0
4.0
2.0
4.0
5.5
6.4
7.2

the South Scotia Ridge--considered to be basic igneous rock by Griffiths and others--could easily extend along the length of the South Scotia Ridge, and, if so, would account for both the aforementioned magnetic configuration and the reported presence of ultrabasic rocks in the basement complex.

Reflection profiling in the Scotia Sea reported by Heezen and Johnson (1965), has revealed a thick (1 km) sedimentary sequence in the concavity behind the South Sandwich Arc, in effect smoothing the bottom topography through burial of basement relief. One might speculate here and attempt to explain the acidic to intermediate nature of the volcanism in the South Sandwich Islands and contiguous East Scotia Basin as the consequence of melting and absorption of part of the sedimentary section during igneous intrusion. Such acidic to intermediate volcanism, coupled with basic intrusion (diking), could also explain the high magnetization contrasts which characterize the numerous magnetic anomalies in the area.

Correlation with Gravity Anomalies

An interesting pattern is immediately discernible in the gravity values reported by Griffiths and others (1965) from the Scotia Sea. Bouguer gravity anomaly values are low (0 - +30 mgal) over the Antarctic Peninsula--as would be expected from a continental section more or less in isostatic equilibrium. However, to the north, across the Bransfield Strait, a Bouguer anomaly high (approximately +130 mgal) is encountered over the South Shetland Islands. Eastward along the South Scotia Ridge the Bouguer anomaly values increase in magnitude

with a maximum of +182 mgal occurring on Gibbs Island, thereafter decreasing slightly in value over the South Orkney Islands. Significantly, the only reported ultrabasic rocks occurring along the South Scotia Ridge crop out on Gibbs Island, where they underlie the schists described as comprising the basement complex of the South Scotia Ridge.

The above relationship also lends credence to the extrapolation of the structure of the Bransfield Strait eastward along the South Scotia Ridge based on the interpretation of the magnetic anomaly configuration as previously discussed. This would also suggest the presence of a core of dense ultrabasic rocks within the full length of the South Scotia Ridge.

Gravity measurements over the South Sandwich Islands reported by Griffiths and others (1965) also seem to substantiate the interpretation of the seismic refraction profiles of Ewing and Ewing (1959). Here the presence of high Bouguer anomaly values (greater than +200 mgal) support their contention that a high-velocity (dense) crustal layer is "arched up" under the South Sandwich Islands.

Bouguer anomaly values similar to those reported from the South Shetland Islands were also reported to occur in South Georgia. Clerke Rocks is the site of the highest Bouguer anomaly (+196 mgal) listed by Griffiths and others (1965) for the North Scotia Ridge. Again, this may be the result of the presence of a dense island core, as postulated for the South Scotia Ridge, but also it could be explained by postulating that a subcrustal structural extension of the South

Sandwich Island Arc occurs there.

To the west of South Georgia a transition must occur, with the dense ridge core--if it is present--being replaced by the low-velocity "sedimentary" section previously discussed as characteristic of Burdwood Bank--which is also suggested by the magnetic anomaly pattern over the area.

Seismicity of the Scotia Sea

An earthquake epicenter chart (Fig. 14) was constructed from data culled from the International Seismological Summary (I.S.S.) from 1936 to 1960 and from the United States Coast and Geodetic Survey Seismological Bulletin from 1960 to 1967. With the start of determining earthquake epicenters by computer in 1956, source locations have become more precise and hence are distinguished in Fig. 14 from those determined prior to that time. U.S.C.&G.S. data for the time since 1960 were readily accessible and contained a greater number of earthquakes analyses than the I.S.S. data. For this reason, and because of the availability of the IBM card format, U.S.C.&G.S. data have been used from 1960 on.

With the advent of the International Geophysical Year in 1957 and of project VELA UNIFORM, a greater density of recording stations was achieved in areas surrounding the Scotia Sea. Increased instrument sensitivity during the same period, coupled with the aforementioned higher station density and computer analysis, allowed greater precision in the determination of earthquake epicenters, focal depth,

Fig. 14. Seismicity of the Scotia Sea. Open squares are earthquake epicenters for 1936-1960, as reported in the I.S.S.; solid squares are earthquake epicenters for 1960-1964, as reported in the I.S.S.; solid circles are shallow-focus epicenters for 1964-1967, as reported by the U.S.C.&G.S.; and solid triangles are intermediate-focus epicenters for 1964-1967, as reported by the U.S.C.&G.S.

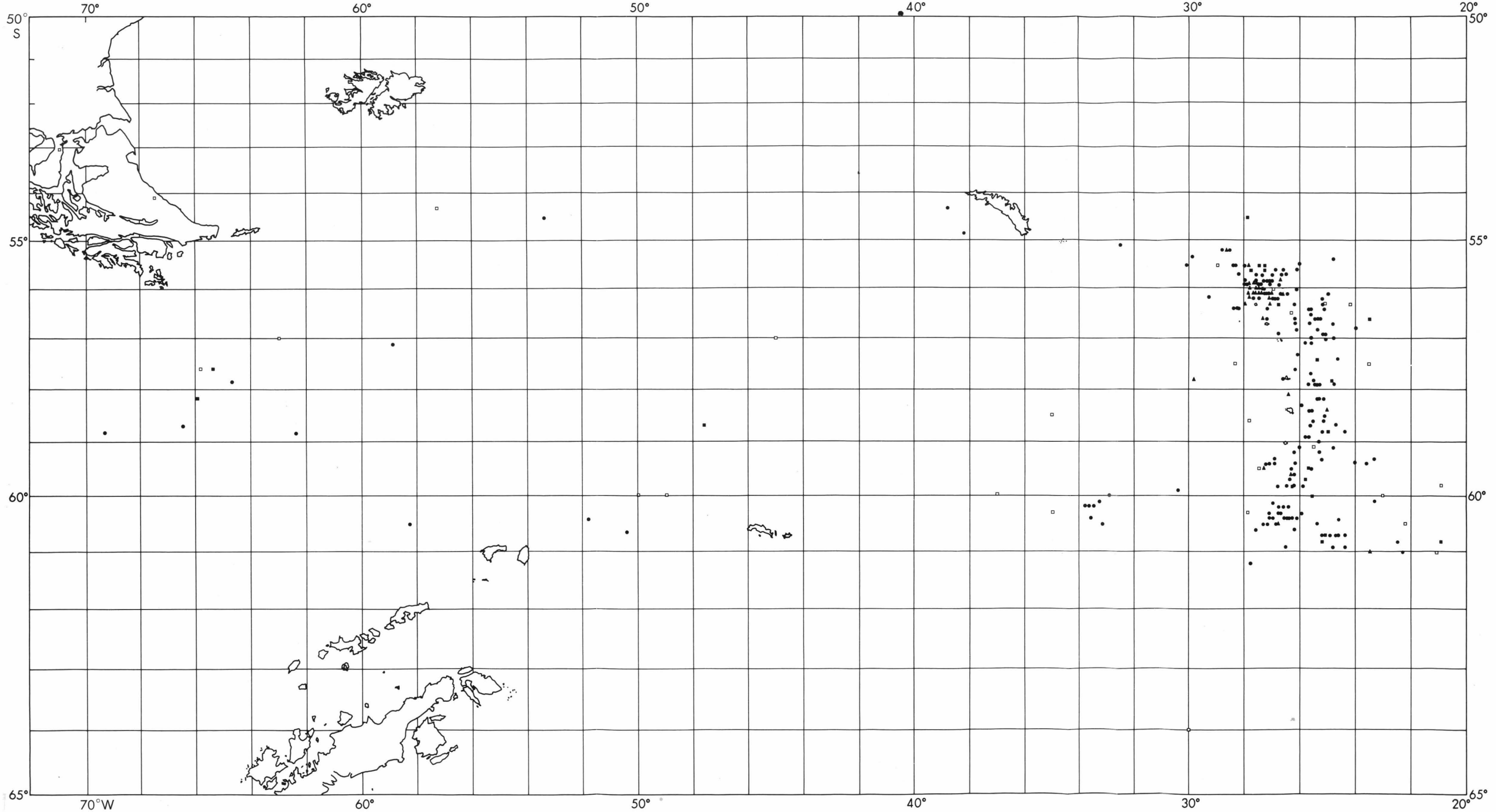
70°
60°
50°
40°
30°
20°
50°
S
55°
60°
65°
70°W
60°
50°
40°
30°
20°
50°
55°
60°
65°

and magnitude. Recently Sykes (1963) has further improved the precision of the determination of the above parameters.

The chart in Fig. 14 differs from the charts of previous writers, such as Gutenberg and Richter (1954) and Heezen and Johnson (1965), in that it includes more events. No attempt was made to recalculate the epicenters as Sykes (1963) has done. More precise determinations are beyond the scope of this paper.

Correlation is observed in Fig. 14 between earthquake activity in the Scotia Sea and structures previously discussed. As indicated by other writers, the volcanically active region (South Sandwich Arc) is also an area of high seismicity. Although the earthquake data do not clearly demonstrate that intermediate focal depths are confined to a zone under the Island arc--which Sykes and Ewing (1965) have shown to be the case in the Caribbean and in other areas--the data do suggest this probability. Interestingly enough, there is a possible correlation between the occurrence of earthquakes and the eastward extension of the South Sandwich Fracture Zone. Similarly, to the north, there also seems to be a concentration of earthquake activity at the intersection of the North Sandwich Fracture Zone and the South Sandwich Arc.

Although earthquake epicenter determinations may be too sparse and too imprecisely determined behind the active arc in the East and West Scotia basins to afford much more than speculation, there appears to be a slight concentration of events within the Drake Passage. This may be significant, considering the previous discussions of magnetic

lineations and bathymetry, and may have implications on the interpretation of the tectonic framework of the region.

TECTONIC FRAMEWORK OF THE SCOTIA SEA--

CONCLUDING REMARKS

It was stated earlier that the most striking aspect of the residual magnetic field chart (Fig. 6) and of the bipole trend chart (Fig. 7) is the convergence of magnetic anomaly lineations within the Drake Passage. This, together with the parallel alignment of anomaly trends with the Scotia Ridge, forms the basis for some intriguing speculation. In the light of recent interest in sea-floor spreading--resulting from the work of Hess (1962), Vine and Matthews (1963), and other workers--two alternative theoretical explanations are offered as a cause of the magnetic anomaly pattern in the Scotia Sea.

1. Possible structural distortion and bending of former north-south anomalies associated with and originating from the East Pacific Rise and resulting from the plastic flow and migration of Pacific crust into the Scotia Sea. In this case, an attempt should be made to explain the apparent absence of magnetic anomaly reversals. One possible explanation would be that the formation of the source for the anomalies occurred during a period when no reversals of the earth's field took place--a conclusion which appears somewhat tenuous, at least in the light of recent studies elsewhere.

2. The formation of east-west shear zones, likewise resulting from the migration of Pacific crust into the Scotia Sea. In this situation the residual magnetic anomaly pattern would be caused by subsequent intrusion and diking within the zones of shear, or from the effects of crustal distortion resulting from folding and buckling

of a thin oceanic crust moving past thick continental salients (Tierra del Fuego and the Antarctic Peninsula) as suggested by Woollard (in press).

Both of these hypotheses appear to explain equally well the anomaly pattern within the confines of the Scotia Sea. However, prerequisite to both hypotheses is an eastward flow of Pacific crust into the south Atlantic; i.e., the Scotia Sea. This idea is not new, having originally been hinted at by Barrow (1831), and recently speculated on by Woollard (in press), who suggests "that the Scotia Arc results from localized crustal migration induced by subcrustal flow in the mantle," without speculating on the mechanism responsible for subcrustal flow. The morphology of the Scotia basins expressed in the bathymetric chart of the Scotia Sea (Fig. 11) together with the seismic refraction results of Ewing and Ewing (1959) tend to confirm Woollard's speculation. The existence of the Scotia Arc and South Sandwich Trench adds further impetus to the idea when examined in the light of Wilson's (1954) theoretical cross-section of a typical active-island-arc, trench system. This idea is even further substantiated by Sykes (1963) and Sykes and Ewing (1965) detailing the attitude of the fault plane dipping under arcs from the trench sides in both the Pacific and Carribbean (the analogy of which is valid for the crustal and upper mantle section even though deep-focus earthquakes are not known to occur in the Scotia Arc). Furthermore, the presence of forerunning eastward extensions of the North and South Sandwich fracture zones may be evidence for an effective channeling of the crust beneath the Scotia Sea during its eastward thrust into the Atlantic.

LITERATURE CITED

Ade-Hall, J. M., 1964, The magnetic properties of some submarine oceanic lavas, Geophys. J., v. 9, p. 85-92.

Adie, Raymond J., 1962, The geology of Antarctica, p. 26-39 In H. Wexler, M. J. Rubin, and J. E. Caskey, Jr., (eds.), Antarctic Research, Am. Geophys. Union Geophys. Mono. No. 7, American Geophysical Union, Washington, D. C.

Anderson, John J., 1965, Bedrock geology of Antarctica: a summary of exploration, 1831-1962, p. 1-70 In Jarvis B. Hadley (ed.) Geology and Paleontology of the Antarctic, Antarctic Res. Ser. Volume 6, American Geophysical Union, Washington, D. C.

Andersson, J. G., 1906, On the geology of Graham Land, Geol. Inst. Upsala Bull., v. 7, p. 19-71.

Atlas Antarktiki, 1966, [Atlas of Antarctica], Vol. 1, Chief Directorate for Geodesy and Cartography, Ministry of Geology of the U.S.S.R., Moscow-Leningrad, 248 pp.

Barrow, John, 1831, Introductory note [to an article on the Islands of Deception], Roy. Geograph. Soc. J., v. 1, p. 62.

Bullard, E. C. and R. G. Mason, 1961, The magnetic field astern of a ship, Deep-Sea Res., v. 8, p. 20-27.

Cox, A. and R. Doell, 1962, Magnetic properties of the basalt in hole EM7, Mohole Project, J. Geophys. Res., v. 67, no. 10, p. 3997-4004.

Driscoll, R. L. and P. L. Bender, 1958, Proton gyromagnetic ratio, Phys. Rev. Letters, v. 1, p. 413-414.

Eltanin Data Sheets, 1962-1963, [on file] National Science Foundation, Washington, D. C.

Ewing, J. and M. Ewing, 1959, Seismic refraction measurements in the Scotia Sea and South Sandwich Island Arc, p. 22-23 In M. Sears (ed.), International Oceanographic Congress Preprints, Am. Assoc. Adv. Sci., Washington, D. C.

Fairbridge, R. W., 1952, The geology of the Antarctic, p. 56-101 In F. A. Simpson (ed.), The Antarctic Today, New Zealand Antarctic Society, Wellington.

Ford, Arthur B., 1964, Review of Antarctic geology, Trans. Am. Geophys. Union I. G. Bull. No. 82, v. 45, no. 2, p. 363-381.

Furumoto, Augustine S. and George P. Woollard, 1965, Seismic refraction studies of the crustal structure of the Hawaiian Archipelago, Pacific Sci., v. 19, no. 3, p. 315-319.

Gass, I. G., P. G. Harris, and M. W. Holdgate, 1963, Pumice eruption in the area of the South Sandwich Islands, Geological Mag., v.100, no. 4, p. 321-330.

Goodell, H. G., [undated ms.], Marine geology of the Drake Passage, Scotia Sea, and the South Sandwich Trench, USNS ELTANIN Marine Geology Cruises 1-8, Florida State University, Dept. Geol., Sedimentology Res. Lab.

Griffiths, D. H., R. P. Riddihough, H. A. D. Cameron, and P. Kennett, 1965, Geophysical investigation of the Scotia Arc, British Antarctic Surv. Sci. Rept. No. 46, 43 pp.

Gutenberg, B. and C. R. Richter, 1954, Seismicity of the Earth, Princeton University Press, Princeton, New Jersey, 310 pp.

Hamilton, Warren, 1963, Tectonics of Antarctica, p. 4-15, In O. E. Childs and B. Warren Beebe (eds.), The backbone of the Americas--

Tectonic history from pole to pole, a Symposium, Am. Assn. Petrol. Geol. Mem. 2.

Hawkes, Donald D., 1962, The structure of the Scotia Arc, Geological Mag., v. XCIX, no. 1, p. 85-91.

Heezen, Bruce C. and G. Leonard Johnson, 1965, The South Sandwich Trench, Deep-Sea Res., v. 12, p. 185-197.

Heezen, B. C. and M. Tharp, 1961, The physiographic diagram of the South Atlantic, the Caribbean, the Scotia Sea, and the eastern margin of the South Pacific Ocean, The Geological Scoeity of America, New York, 1 sheet.

Heezen, B. C., M. Tharp, and M. Ewing, 1959, The floors of the oceans: I, The North Atlantic, Geol. Soc. Am. Spec. Paper 65, 122 pp.

Herdman, H. F. P., 1932, Report on soundings taken during the DISCOVERY investigations, 1926-1932, Discovery Reports, VI, p. 205-236.

Herdman, H. F. P., 1948, Soundings taken during the DISCOVERY investigations, 1932-1939, Discovery Reports, XXV, p. 39-106.

Hess, H. H., 1962, History of ocean basins, p. 599-620 In Petrologic Studies--A volume in honor of A. F. Buddington, The Geological Society of America, New York.

Hirshman, J. and B. Luskin [unpublished ms.], A two-conductor Proton Precession Magnetometer for marine use, Lamont Geological Observatory, New York.

Holtedahl, Olaf, 1929, On the geology and physiography of some Antarctic and sub-Antarctic islands, Scientific Results Norwegian Antarctic Expedition, 1927-1929, No. 3, Norske videnskajos-akademi, Oslo, 172 pp.

International Seismological Summary, The, 1939-1960, Kew Observatory, Richmond, Surrey, England.

Kroenke, Loren W. and George P. Woollard (in prep.), Geomagnetic investigations in the Labrador and Scotia seas, USNS ELTANIN cruises 1-10, 1962-1963, Hawaii Inst. Geophys. rept. HIG-68-4.

Lamont Geological Observatory, 1963-1965, Precision depth recorder soundings, USNS ELTANIN cruises 4-10, 1962-1963, [on file] Columbia University, New York City.

Lincoln, J. Virginia, 1962-1964, Geomagnetic and solar data, J. Geophys. Res., v. 67, no. 6 to v. 69, no. 9, various pp.

Luyendyk, Bruce P. and William G. Melson, 1967, Magnetic properties and petrology of rocks near the crest of the Mid-Atlantic Ridge, Nature, v. 215, p. 147-149.

Malahoff, Alexander and G. P. Woollard, 1966, Magnetic surveys over the Hawaiian Islands and their geologic implications, Pacific Sci., v. 20, no. 3, p. 265-311.

Matthews, D. H., 1959, Aspects of the geology of the Scotia Arc, Geological Mag., v. XCVI, no. 6, p. 425-441.

Matthews, D. H., 1961, Lavas from an abyssal hill on the floor of the Atlantic Ocean, Nature, v. 196, no. 4771, p. 158-159.

Matthews, D. S., 1939, Tables of velocity of sound in pure water and sea water for use in echo-sounding and echo-ranging, Admiralty Hydrographic Department, London, 52 pp.

Maurer, H. and T. Stocks, 1933, Die echolotungen des Meteor, Wiss. Ergebn. d. Deutsch. Atlant. Exped. METEOR 1925-1927, v. 11, p. 1-309, Berlin and Leipzig.

Nagata, Takesi, 1961, Rock Magnetism, 2nd ed., Maruzen Company, Tokyo, 350 pp.

Nelson, J. H., 1960, The gyromagnetic ratio of the proton, J. Geophys. Res., v. 65, no. 11, p. 3826.

Nettleton, L. L., 1940, Geophysical Prospecting for Oil, McGraw-Hill Book Company, Inc., New York, 444 pp.

Nordenskjöld, Otto, 1910, Die geologischen beziehungen zwischen Südamerika und der angrenzenden Antarktika, Intern. Geol. Congr. 11th (Stockholm, 1905), Compt. Rend., p. 759-765.

Ostenso, Ned A., 1962, Geophysical investigations of the Arctic Ocean basin, University of Wisconsin Geophysical and Polar Research Center, Research Report Series No. 62-4.

Peters, L., 1949, The direct approach to magnetic interpretation and its practical applications, Geophysics, v. 14, p. 290-320.

Sankar-Narayan, P. V., 1961, Mathematical methods in the interpretation of magnetic data, University of Wisconsin, unpublished Ph.D. thesis.

Seismological Bulletin, 1960-1967, U. S. Coast and Geodetic Survey, MSI 312, Washington, D. C.

Stocks, Th., 1937, Morphologie der Atlantischen Ozeans, Part IV (1), Grund-Karte der Ozeanischen Lotungen, 1:5 millionen, Blatt SII_2, Wiss. Ergebn. d. Deutsch. Atlant. Exped. METEOR 1925-1927, III, Part I, 1 chart, Berlin and Leipzig.

Suess, E., 1909, Das Antlitz der Erde, G. Freytag, Leipzig, p. 553-559. [(translation) The Face of the Earth, Vol. 4, Clarendon Press, Oxford, 673 pp.]

Sykes, Lynn R., 1963, Seismicity of the South Pacific Ocean, J. Geophys. Res., v. 68, p. 5999-6006.

Sykes, Lynn R. and Maurice Ewing, 1965, The seismicity of the Caribbean region, J. Geophys. Res., v. 70, no. 20, p. 5065-5074.

Tilley, C. E., 1930, Petrographical notes on rocks from Elephant Island, South Shetlands, Report on the Geological Collection Made During the Voyage of the QUEST on the Shackleton-Rowett Expedition to the South Atlantic and Weddell Sea in 1921-1922, British Museum Nat. Hist., London, p. 56-62.

Tilley, C. E., 1935, Report on rocks from the South Orkney Islands, Discovery Reports, X, p. 383-390.

Trendall, A. F., 1953, The geology of South Georgia--I, Falkland Islands Dependencies Survey Scientific Reports No. 7, 26 pp.

Trendall, A. F., 1959, The geology of South Georgia--II, Falkland Islands Dependencies Survey Scientific Reports No. 19, 48 pp.

Tyrrell, G. W., 1921, A contribution to the petrography of the South Shetland Islands, the Palmer Archipelago, and the Danco Coast, Graham Land, Antarctica, Trans. Roy. Soc. Edinburgh, v. 53, pt. 1, no. 4, p. 57-79.

Tyrrell, G. W., 1930, The petrography and geology of South Georgia, Report on the Geological Collection Made During the Voyage of the QUEST on the Shackleton-Rowett Expedition to the South Atlantic and Weddell Sea in 1921-1922, British Museum Nat. Hist., London, p. 28-54.

Tyrrell, G. W., 1945, Report on rocks from West Antarctica and the Scotia Arc, Discovery Reports, XXIII, p. 37-102.

U. S. Naval Oceanographic Office, 1955, The total intensity of the Earth's magnetic force, [U. S. Hydrographic Office] Chart H. O. 1703, U. S. Government Printing Office, Washington, D. C.

U. S. Naval Oceanographic Office, 1961, The world, [U. S. Hydrographic Office] Chart H. O. Miscellaneous 15,254-11, U. S. Government Printing Office, Washington, D. C.

U. S. Naval Oceanographic Office, 1965, The magnetic inclination or dip for the year 1965, Chart No. 1700, U. S. Government Printing Office, Washington, D. C.

U. S. Naval Oceanographic Office, 1965, The total intensity of the Earth's magnetic force, Chart No. 1703, U. S. Government Printing Office, Washington, D. C.

Vacquier, V., N. C. Steenland, R. G. Henderson, and I. Zietz, 1951, Interpretation of aeromagnetic maps, Geol. Soc. Am. Mem. 47, 151 pp.

Vine, F. J. and D. H. Matthews, 1963, Magnetic anomalies over ocean ridges, Nature, v. 199, no. 4897, p. 947-949.

Vogt, Peter R. and Ned A. Ostenso, 1966, Magnetic survey over the Mid-Atlantic Ridge between 42°N and 46°N, J. Geophys. Res., v. 71, no. 18, p. 4389-4411.

Waters, G. S. and P. D. Francis, 1958, A nuclear magnetometer, J. Sci. Instr., v. 35, no. 3, p. 88-93.

Wilson, J. Tuzo, 1954, The development and structure of the crust, Chapt. 4, p. 138-214 In Gerard P. Kuiper (ed.), The Solar System: II, The Earth as a Planet, University of Chicago Press, Chicago.

Wold, Richard J. and Thomas R. Wolfe, 1966, Computer methods of analyzing aeromagnetic data, University of Wisconsin Geophysical and Polar Research Center, Research Report Series No. 66-1.

Woollard, G. P. (in press), The geology of Antarctica [in a monograph on Antarctica], Scott Polar Research Institute, Cambridge, England.

Except as otherwise noted, copies of all publications listed here are distributed free of charge, as long as available.

Address all requests for publications to:

Publications, Room 262
Hawaii Institute of Geophysics
University of Hawaii
2525 Correa Road
Honolulu, Hawaii 96822

**Out of print*